Electrical Bioimpedance as a detection tool for internal hemorrhaging and blood aggregation

John Morse

A thesis submitted to the

Faculty of Graduate and Postdoctoral Studies

in partial fulfillment of the requirements for the

MASc degree in Biomedical Engineering

Department of Biomedical Engineering

Faculty of Engineering

University of Ottawa

Contents

List of Tables

List of Figures

Abstract

Electrical bioimpedance was used to detect local volume and aggregation changes in blood. This was done with two separate experimentation processes to improve upon current research methods.

Abdominal internal hemorrhaging is bleeding and pooling of blood within the abdominal cavity which can put the welfare of the patient at risk and may cause organ failure. Electrical bioimpedance is the response of biological tissue to applied electrical current. In cooperation with Bioparhom, electrical bioimpedance was used as a detection device for abdominal internal hemorrhaging. It is hypothesized that electrical bioimpedance could be a non-invasive and cost effective avenue for the detection of internal bleeding. In this study we investigate the use of electrical bioimpedance with a custom 8x8 needle electrode array, for detecting and locating the blood pooling due to a drop in resistivity in a rat using a *Z-Metrix* (function generator by Bioparhom). 5 and 95 kHz signals were inputted into a dead rat experiencing internal bleeding of porcine blood at a rate of 3.33 ml/min to 10 ml. For 8 rats, the 5 kHz frequency was found to be more sensitive to internal blood pooling.

Red blood cell aggregation is a physiological process where red blood cells form reversible aggregates. RBC aggregation is an important indicator for physicians for the health of the circulatory system. Utilizing electrical bioimpedance, it is hypothesized that a reactance change as a result of blood aggregation will be detected. As well, a method is developed using impedance spectroscopy to determine s frequency which exhibits the highest reactance change during blood aggregation. This sensitive frequency, found to be 304 kHz, is compared to a frequency used by previous studies (100 kHz) to validate its. Using the *Z-Metrix* (function generator by Bioparhom) with a custom 4 electrode configuration, 2 ml of porcine blood mixed with 2 mg/ml of EDTA is

tested for 2 minutes at a single frequency. The 304 kHz is found to be the most sensitive of the frequencies tested to reactance changes during aggregation. Results found for blood samples give an average AI_c of 27.32 ± 11.44, which is within the physiological range for porcine blood of 3-30. It is seen that the 304 kHz has a higher precision than the 100 kHz frequency, but the AI_c is within the same magnitude. As a result, 304 kHz is found to be a more favorable frequency than the previously published 100 kHz for the trials performed based on precision of the results and the sensitivity of the reactance change to blood aggregation.

Glossary and definitions

AI	Aggregation Index for Light Transmittance
AI_c	Aggregation Index modified for Capacitance
C	Capacitance
EIT	Electrical Impedance Tomography
H	Hematocrit (or packed cell volume), percentage of the blood occupied by the red blood cells
LT	Light Transmittance
R	Resistance
RBC	Red Blood Cell
SD	Standard Deviation
Z	Impedance

1 Introduction

Electrical bioimpedance is the response of biological tissue to applied electrical current. Bioimpedance is simply the measurement of electrical resistance and reactance. Bioimpedance allows for measurements of electrical properties to be taken in a non-invasive fashion, rapidly and at low cost. This principle has been in practice for 40 years, since which numerous studies have been performed in efforts to develop non-invasive medical diagnostic methods [1]. The used of bioimpedance was limited for many years due to difficulties with the technology. In the last two decades, interest in bioimpedance has grown due to advances in the technology and signal processing algorithms, making bioimpedance ideal for several biological measurements. Some examples are for total body composition measurements, such as percent total body water and fat content, for cardiac output measurements, for water volume monitoring during dialysis treatment or plethysmography. The objective is to improve upon and develop new applications, using bioimpedance; creating tools to assist medical professionals.

In this context Bioparhom, a medical device company based out of Bourget du lac, France, approached us to explore new diagnostic capabilities for their Z-Metrix. The company designed the Z-Metrix, a professional electrical bioimpedance meter and the Z-Eval, a body composition evaluation service. The Z-Metrix is an ISO 13485 device certified for tissue, fluid and metabolic indicators. We partnered with Bioparhom to use their Z-Metrix as a bioimpedance function generator and data acquisition system, with the goal of expanding its diagnostic capability with fluid indicators, in particular the detection of internal hemorrhaging and the measurement of blood aggregation

Internal bleeding, is any bleeding found within the human body. The bleeding becomes more dangerous when located within a major cavity (cranial, thoracic or abdominal). Current detection methods are lacking in their price, portability or accuracy. Electrical bioimpedance could be a non-invasive and cost effective promising avenue for the detection of internal bleeding. We hypothesize that bleeding near the

electrical current path should display a decrease in resistance at low frequencies using electrical bioimpedance.

Blood aggregation is a reversible stacking of red blood cells, similar in shape to a roll of coins. Aggregation is an indicator for several blood ailments, such as sepsis. The gold standard sedimentation test, to measure blood aggregation, requires several hours to run. This length of time can be costly for blood ailments which require rapid application of the appropriate treatment. The Z-Metrix will be tested to detect blood aggregation using a smaller window of time, on the order of minutes. Using electrical bioimpedance, we expect that the aggregation of blood changes the reactance of the solution for a given cross-section. As blood aggregates, we hypothesize that the reactance should begin to drop, and using modified methods already in practice, an aggregation index will be found.

We hypothesize that the use of electrical bioimpedance measurements from the Z-Metrix is capable of detecting the macro changes in the resistance of the abdominal cavity caused by internal bleeding as well as the micro changes in the reactance of a blood sample due to blood aggregation.

Chapter 2 discusses the theory of electrical bioimpedance, and the methods associated with it. The electrode set-up is also discussed, and it will introduce the electrical properties of blood. Chapter 3 introduces the topic of internal hemorrhaging and the current state of detection methods. After providing some background literature, a novel approach to the use of electrical bioimpedance in measuring internal bleeding is proposed. The results and conclusions associated with the approach are shown. Lastly, Chapter 4 reviews the topic of blood aggregation and the aggregation index as a diagnostic tool for clinicians. Improving upon the sedimentation method, and altering formulae used in research, an electrical bioimpedance set-up is presented. After the results and conclusions are presented for blood aggregation, Chapter 5 gives the overall conclusions of the research.

The unique contributions are the development of a method to perform electrical bioimpedance experiments for blood aggregation and pooling using the Z-Metrix, a clinically certified device. Finding an appropriate frequency to work with for each experiment, and comparing it to the current standard was also done.

2 Electrical Bioimpedance

2.1 Electrical Bioimpedance

Electrical impedance is the use of an applied voltage to a circuit to measure its resistance to the current. The impedance measurement provides the complex ratio of reactance and resistance for the circuit. Electrical bioimpedance occurs when the applied current enters biological tissues or systems.

Utilizing the ability to measure complex impedance ratios, applying small electrical currents to biological tissue can give the output impedance measured across the biological system. Additionally, varying the frequency of the signal will give differing values and provide a way to measure and compare the capacitance and resistance effects individually. At low frequencies, the current is unable to enter the cell and only measures the extracellular fluid resistance, whereas at higher frequencies the current can enter the cell and measures both intra and extracellular resistances. The path of the electrical current in biological tissue can be seen in Figure 1.

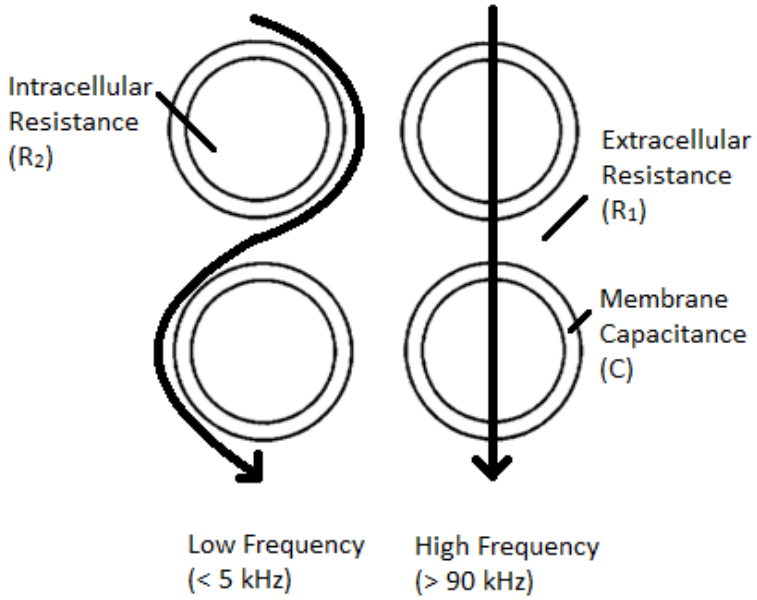

Figure 1 Diagram showing the current paths at different frequencies and the circuit model components. Modified from [2].

Circuit models were proposed to determine the values of each of the elements [2]. The models defines how each of the elements act, in which order the elements are placed, and their magnitudes.

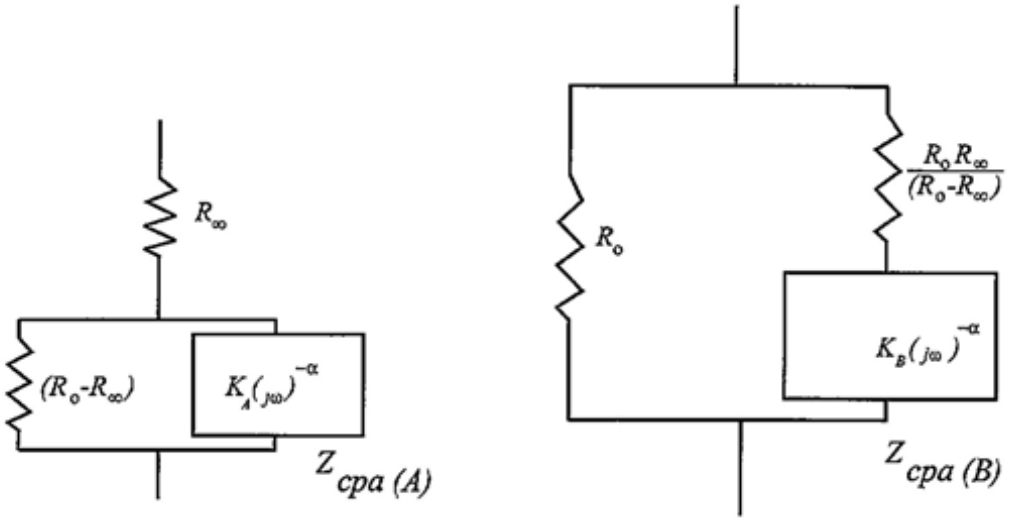

Figure 2 Two different circuit models representing the same system. The values of the internal components change but the overall circuit impedance does not [3].

Figure 2 shows circuit models for biological tissue. These models can be used to compute the values of constituents. The measurement would give either an indication about the system (such as body water content, cell content etc.) or the time dependent change of impedance (for example the liquid volume change). Figure 3 shows the imaginary value (reactance) as a function of the frequency. At low frequencies, the capacitance or reactance has little impact on the impedance since the current cannot pass through the cell. As the frequency increases, the reactance has more of an impact as more of the current enters the cell. Eventually, a high enough frequency is reached where the current enters the cell with little impedance and the reactance again has little impact on the impedance. A graph showing this trend is typically called a Cole-Cole plot [4].

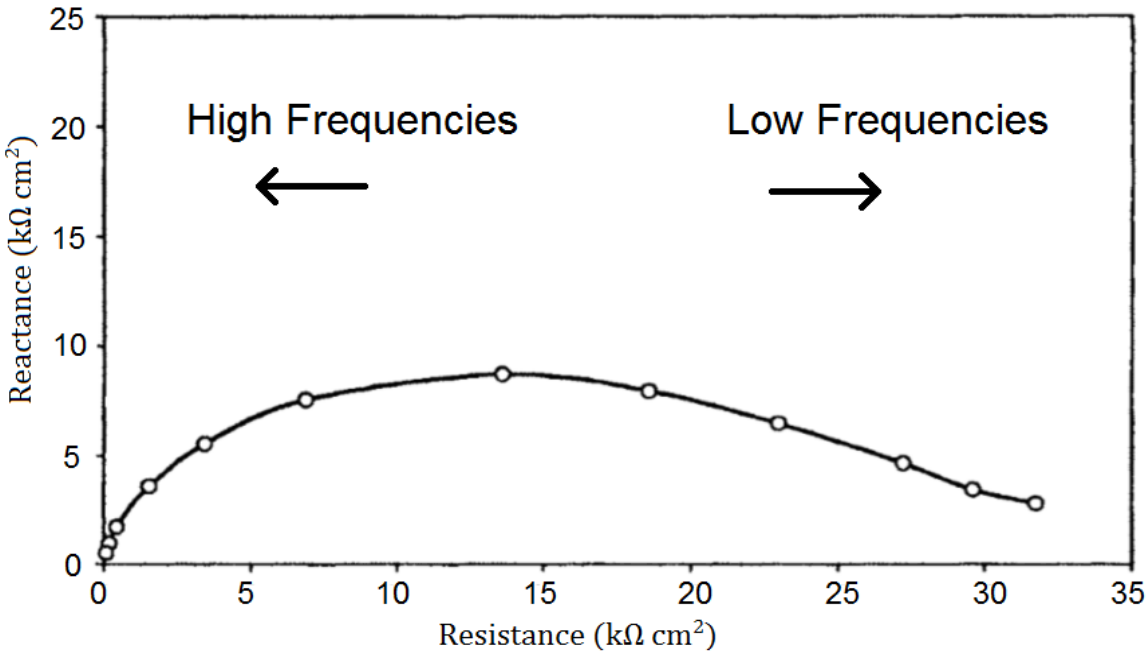

Figure 3 Cole-Cole plot, modified from [1].

For measurements relying largely on resistance, or change in resistance, a low frequency is more useful. At lower frequencies, the impact of resistance is enhanced since the capacitance becomes an open circuit so all of the current is forced through the resistors. Based on this, a slight change in resistance will drastically change the output impedance. A typical value for this is around or below a frequency of 5 kHz for biological tissue.

The choice of frequency is application dependent, for example to investigate extracellular water content a low frequency signal is more appropriate. This is because the signal will not penetrate the cell wall, due to the membranes capacitance. For intracellular water content, a higher frequency is more appropriate since it allows the current to penetrate into the cell.

2.2 Electrical Bioimpedance of Blood

The electrical response of biological tissue has been studied for over 100 years. The advent of better technology has increased the accuracy of many results; however most of the basic principals were developed in the early 1900's and still hold today.

In 1910, *Hober* first looked at the electrical impedance of red blood cells and found that its impedance varied with frequency [5]. He found at low frequencies, the blood had a high resistance (1000 Ω·cm), while at higher frequencies it dropped to a resistance similar to 0.4% NaCl solution (200 Ω·cm). 15 years later, *Fricke and Morse* (1925) developed a model which theorized the electrical resistance of spherical objects suspended in a fluid [2]. This model, shown in Figure 4, accurately fitted blood cells suspended in plasma.

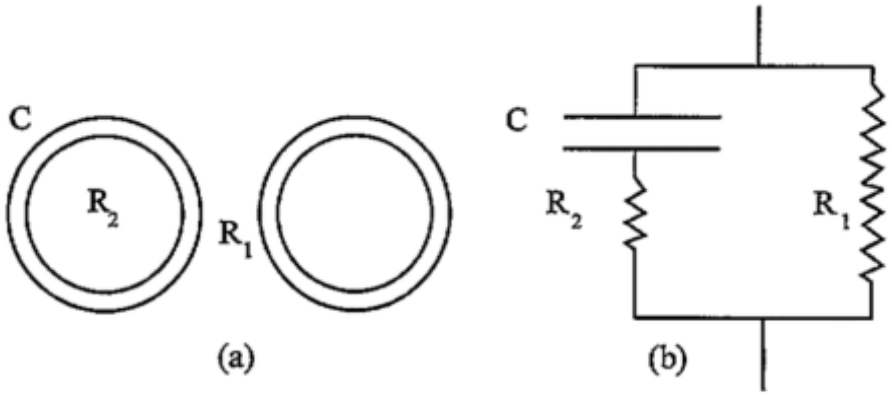

Figure 4 The equivalent circuit model of Fricke and Morse [2] representing the electrical properties of suspended blood cells reproduced from [3].

This work was later take up by *Cole* in 1928 [4], who showed the complex impedance plot for suspended particles. This Cole-Cole plot showed the changes in resistance and reactance as a function of the frequency. An example of a Cole-Cole plot can be seen in Figure 3 of section 2.1.

There are some clinical applications of electrical bioimpedance currently in development and in practice based of bioimpedance properties of the blood. [1]. Impedance plethysmography measures a volume. Dynamic impedance plethysmography is used to measure the changes in volume, such as the volume changes of a beating heart. This method can also be used to measure cardiac output in a limb by constricting the veins in the limb, this causes all of the blood to remain in the limb and a blood flow value can be estimated from volume change. In the 1990s, work started on detecting blood volume changes and pericardial effusions for cardiac measurements [6]. In the early 1990's experimentation began on the detection of internal hemorrhaging using electrical bioimpedance, based on the work done 60 years earlier. A few groups out of Australia [7], Denmark [8], China [9] and Israel [10] have all done research on the measurement and quantification of internal bleeding using electrical bioimpedance.

More recently, a group in Turkey has done research on micro scale electrical bioimpedance trying to measure the aggregation rate and index of blood [11].

2.3 Electrode Configuration

The placement and configuration of electrodes for experimentation is important for accurate bioimpedance measurements. The placement of the electrodes and their configuration affect the depth explored, the sensitive depth and the effect of the electrode contact. The depth explored is a function of the distance between the current-injecting electrodes [1]. This effect can be seen in Figure 5. The depth explored equals roughly half the distance between the current-injecting electrodes [12].

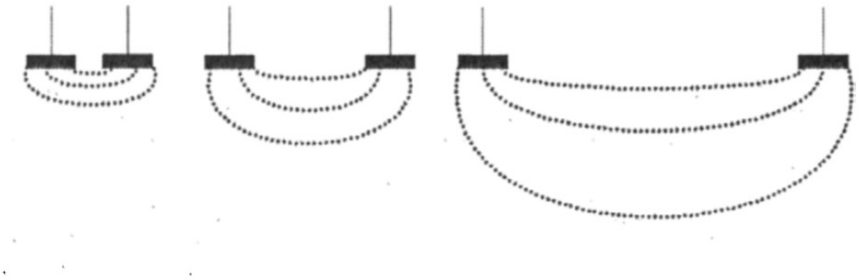

Figure 5 The effect of electrode distance on the depth explored, reproduced from [1]. The dotted lines represent the theoretical path taken by the current.

The sensitivity to the depth depends more on the number of electrodes used, than the spacing of the electrodes. A 3 electrode configuration, as shown in Figure 6, is an electrode configuration that allows 1 lead (R) to measure the current loop made by two electrodes (C and M). This setup is sensitive to the proximal effects, meaning it exaggerates the tissue found closest to the electrodes. A 4 electrode configuration, shown in Figure 7, uses 2 leads (R and R') and measures the segment of tissue between the leads. This segmental focus minimizes the effects of the tissue near the electrode and emphasizes the tissue between the electrodes.

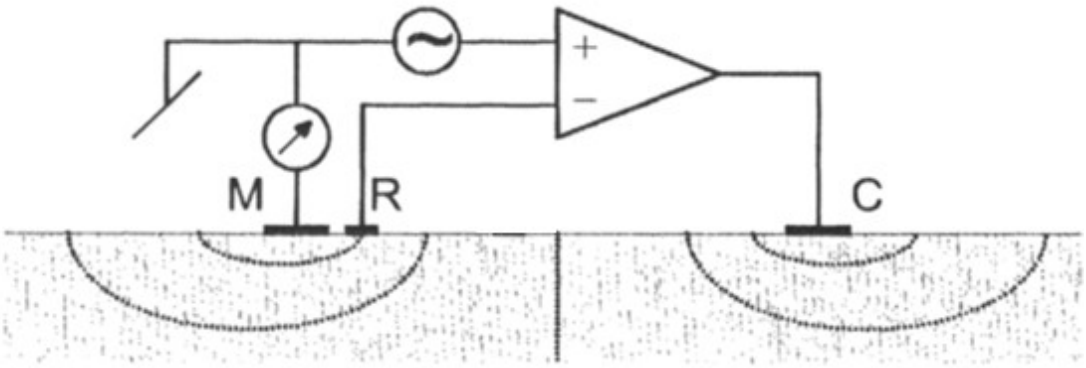

Figure 6 A 3 electrode configuration with C being a current-injecting electrode, R being a lead and M being a current-injecting and recording electrode, modified from [1].

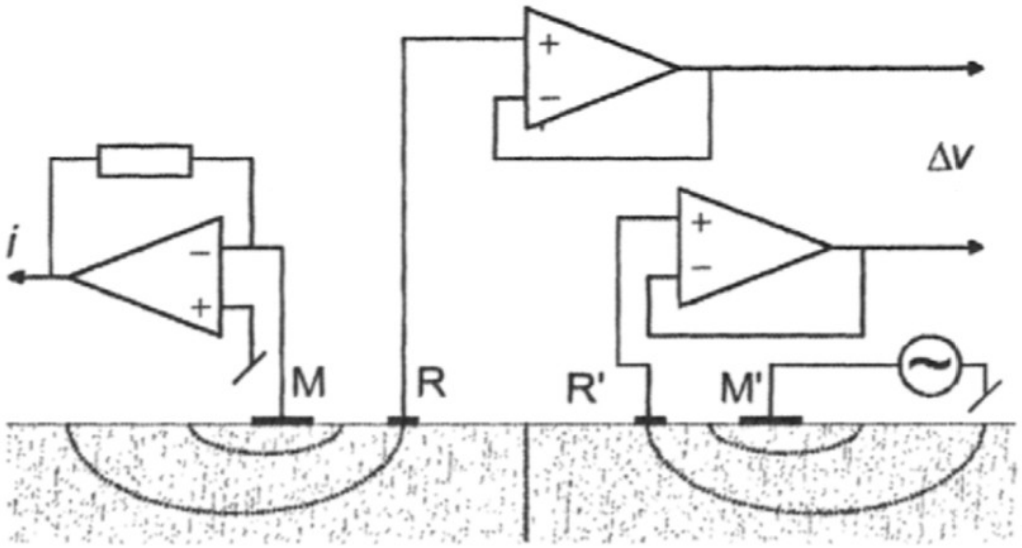

Figure 7 Schematic of a 4 electrode set-up with M and M' being the current-injecting electrodes while R and R' are the leads, reproduced from [1].

In this work we use a bipolar current-injecting electrode configuration with 2 recording leads placed equidistant between the electrodes. The set-up can be seen in Figure 8.

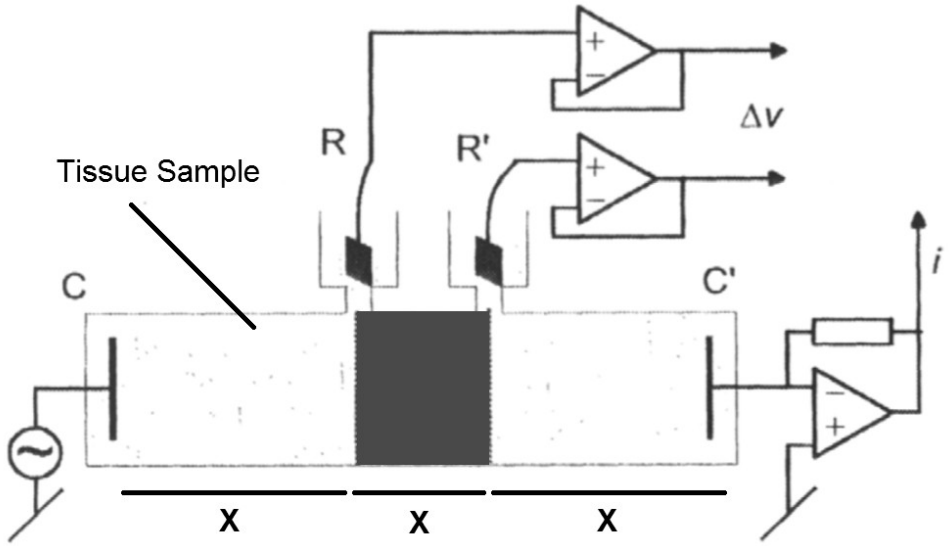

Figure 8 The 4 electrode set-up with the red area being the measured segment, and the X's demonstrate the equidistant spacing of the electrodes. Modified from [1].

The advantage of the 4 electrode set-up is its ability to minimize the tissue near the electrodes and measure the section of tissue between the leads.

2.4 Blood Impedance Properties

The bulk electrical properties of human blood and porcine blood are similar. There is an increased amount of experiments performed using pigs due to their hematological and anatomical similarities to humans [13].

The values for human blood and porcine blood around 25 kHz follow a similar curve. The similarities can be seen in Figure 9. The plot shows the logarithmic curves of human and porcine blood at 37 ^{0}C. They follow similar trends up to a hematocrit of 60, where the curves begin to diverge. Physiological hematocrits for humans and pigs are around 40 [14].

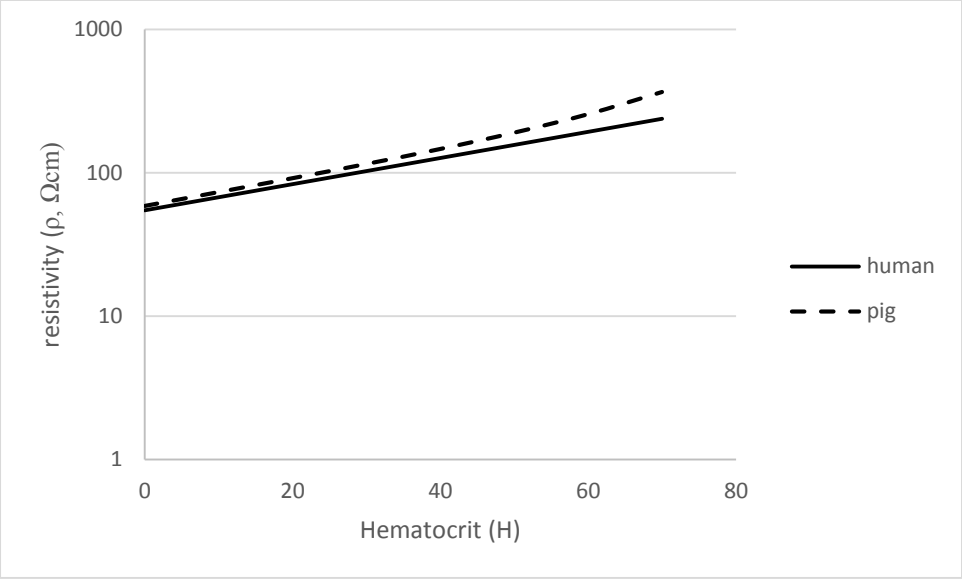

Figure 9 Plot of the resistivity (ρ) as function of hematocrit (packed-cell volume: H) for human and pig blood. Human blood resistivity (logarithmic scale) at 37 ^{0}C using 25 kHz frequency reproduced from [13], porcine blood resistivity (logarithmic scale) at 37 ^{0}C and using between 20 and 50 kHz reproduce from [15].

Calculating the data at all the major hematocrits we get the following table.

Table 1 Comparison of the blood resistivity for human and pig blood with percent error [16] [15].

Hematocrit	**Human blood resistivity (Ω·cm) at 25 kHz**	**Porcine blood resistivity (Ω·cm) at 20-50 kHz**	**Difference (%)**
10	67.48219	73.25	8.5
20	83.2513	91.5625	10
30	102.7053	115.1071	12
40	126.7053	146.5	15.6
50	156.3135	190.45	21.8

The difference between human and porcine blood presented within Table 1 can be explained partially because the frequency used for the pig blood was not the exact same as that used on the human blood. The different frequency used for porcine blood could raise or lower the resistivity depending on the frequency used (in this case 20-50 kHz for porcine blood is compared to 25 kHz results for human blood). At the lower end (20 kHz), we would expect a higher resistivity since the frequency is below that if the human blood (25 kHz). While at 50 kHz, the resistivity of porcine blood would be lower. In addition, considering that porcine's RBCs are smaller than human's RBC, for the same hematocrit, the RBCs are more numerous in the porcine blood. In consequence we can reasonably attribute a part of the difference to the cell volume difference.

3 Internal Hemorrhaging

Abdominal internal hemorrhaging is bleeding and pooling of blood within the abdominal cavity. As a result of the bleeding, the welfare of the patient is at risk and organ failure may occur due to hypoxia. Low systemic blood pressure can also lead to patient death since the blood is pooling outside of the vasculature. Current detection methods for internal bleeding have drawbacks in cost, portability and ease-of-use which warrant research into a new method. It is hypothesized that Electrical bioimpedance could be a non-invasive and cost effective promising avenue for the detection of internal bleeding. In this study we investigate the use of electrical bioimpedance with an 8x8 needle electrode array, for detecting and locating the blood pooling due to a drop in resistivity in a rat. Using a Z-Metrix, a stainless steel 8x8 needle electrode array and a multiplexer, 5 and 95 kHz signals were inputted into a dead rat experiencing internal bleeding of porcine blood at a rate of 3.33 ml/min to 10 ml. For 8 rats, the 5 kHz frequency was found to be more sensitive to internal blood pooling.

3.1 Background

3.1.1 Internal Hemorrhaging

Internal hemorrhaging is any bleeding found within the body. For the purpose of this research, only internal hemorrhaging found within a major body cavity will be discussed with a focus on bleeding in the abdominal cavity.

The presence of internal bleeding causes hypoxia, low levels of oxygen. The blood pooling prevents blood from being distributed to those tissues and organs which need the oxygen due to the pooling of blood outside of the vessels. This lack of blood delivery can cause irreparable organ damage.

Internal bleeding also causes localized high pressure which puts undue strain on nearby organs. This strain can damage the organs by impeding the blood flow to them, or physically damaging the organ.

Internal hemorrhaging is commonly found in patients already suffering from other medical issues aside from internal hemorrhaging. The main causes are trauma (which is generally accompanied by fractures and concussions) and cancer. Trauma causes the rupture of a healthy vessel due to an applied external force. Sometimes these are easy to locate due to bruising which will occur under the skin where the impact happened. In this case, the emergency team can reasonably locate the bleeding under that region of bruising in order to stop it before more damage is done. This is not always the case though as the bruise can be deep and hidden or the damage can occur without bruising. Bleeding found deep within a cavity will not show signs on the surface of the body and as a result other methods of detection would be useful.

The medical symptoms of internal bleeding are non-specific and sometimes difficult to diagnose. Since the loss of blood can lead to death it is imperative for doctors to discover internal bleeding quickly. After around 1 litre of blood lost in a patient, visible symptoms appear such as pale clammy skin and loss of consciousness, which are also symptoms for shock.

Cancer is the other leading cause of internal hemorrhaging. The growth of tumors causes the branching of new blood vessels. The blood vessels stretch and tear as the tumor continues to grow. This is a common concern for bowel and colon cancers, but can occur in other types as well. The danger of this type of internal hemorrhaging is that there is no traumatic event that caused it, and there are rarely nerve cells present close enough for the patient to detect the rupture. Due to this lack of sensation, the patient does not even realize the bleeding is happening until symptoms present themselves. This suggests that there is need for a simple device which can be applied externally to rapidly probe for internal bleeding and locate where it is occurring.

3.1.2 Current Internal Bleeding Detection Methods

There are several detection methods for internal hemorrhaging, yet each has at least one drawback.

The emergency diagnostic method, observed assessment, depends on a medical practitioner to examine the displayed conditions of the patient to interpret and determine the ailment and its location. Displayed conditions are what the patient presents to the medical care provider. This method has no additional costs. The drawbacks are the ambiguous nature of the symptoms, the reliance on an individual human assessment prone to inconsistencies and the amount of bleeding required before symptoms are present. For intra-abdominal bleeding, the symptoms can be:

- Pain
- Bruising if located near the skin
- Weakness
- Lightheadedness
- Shortness of breath
- Clammy skin
- Dizziness or fainting
- Low blood pressure [17]

These symptoms are not unique to internal bleeding in the abdomen, and many are shared with shock and other trauma related ailments, making it difficult to identify internal hemorrhaging in a patient who has suffered a traumatic event. As well, in order for many of these symptoms to present themselves, a large volume of blood loss is required, generally greater than 1 liter for an average adult. Hence, observed assessments are not ideal for diagnosing and locating internal hemorrhaging.

The second method of detecting internal bleeding is ultrasound technology. Ultrasounds may be used to detect the location of blood pooling in the abdomen. It relies on the differences in density of blood and the surrounding tissue. On an ultrasound, blood appears as a void. Ultrasounds are particularly useful for gynecological bleeding detection, since the location of the bleeding is generally known, so the physician only needs to know the severity [17]. Ultrasound technology has advanced over the last few

decades to the point where they are now small, portable and inexpensive medical devices. However they can misdiagnose or lose accuracy in patients who are overweight or obese due to attenuation of the sound waves. The buildup of fat near the skin can interfere with the ultrasound waves [18]. Thin sheets of blood can go undetected by ultrasound. As well, in order to properly read an ultrasound, the user needs extensive training. The extensive training required makes it difficult for first responders to properly diagnose the internal bleeding. Hence ultrasounds are not an ideal solution for diagnosing internal bleeding.

The third method of detecting internal bleeding is Computerized Tomography (CT) scans. These are commonly used to diagnose internal hemorrhaging. CT scans give an accurate picture of what is currently within the body, allowing for easy location and estimation of size of the internal bleeding. They are primarily used for diagnosing cranial bleeding, however they can be used for internal hemorrhaging found elsewhere [17]. CT scans require a large investment from the medical center where they are used. CT scanners have dedicated rooms and specialized technicians to operate them. The costs of the scanner is usually in the hundreds of thousands of dollars, add on a dedicated room with special ventilation and the technology can reach well over $1,000,000 in investment [19]. As a result of the cost associated with CT scanners, only large centralized medical facilities have the means to support one. CT scanners are not portable, and while the scan is occurring, no other procedures can take place. Its stationary nature means first responders and emergency medical personnel will not have access to a CT scanner on short notice. A more accessible and affordable technology for the detection and localization of internal hemorrhaging is needed.

The issues associated with each of these common detection methods creates a need for a new simple, effective, inexpensive and portable detection technique. The method of electrical bioimpedance allows for miniaturized form factors with low costs. The simplicity of use depends on the algorithms and

software used more than the technique. As a result, electrical bioimpedance has the potential to solve the issues with current internal hemorrhaging detection devices.

3.1.3 Effects of Bleeding on Electrical Bioimpedance

Electrical bioimpedance as a measuring tool for internal bleeding may be effective based on the average resistance of blood compared to normal tissue. Depending on the frequency, the average resistance is around 5 Ω·m (abdominal tissue) while blood is around 1.5 Ω·m [20]. This shows a decreased resistance for blood, at around one third normal abdominal tissue. A graphical representation of this is seen in Figure 10. The primary difference is caused by the conductivity of plasma in the blood. Plasma is essentially a saline solution and therefore conducts current with little impedance.

We hypothesize that the primary source of the low impedance is the low resistance of the plasma which will provide the largest change in measured abdominal resistance, it follows that a lower frequency would be more sensitive to changes caused by the introduction of a pool of blood in a body cavity.

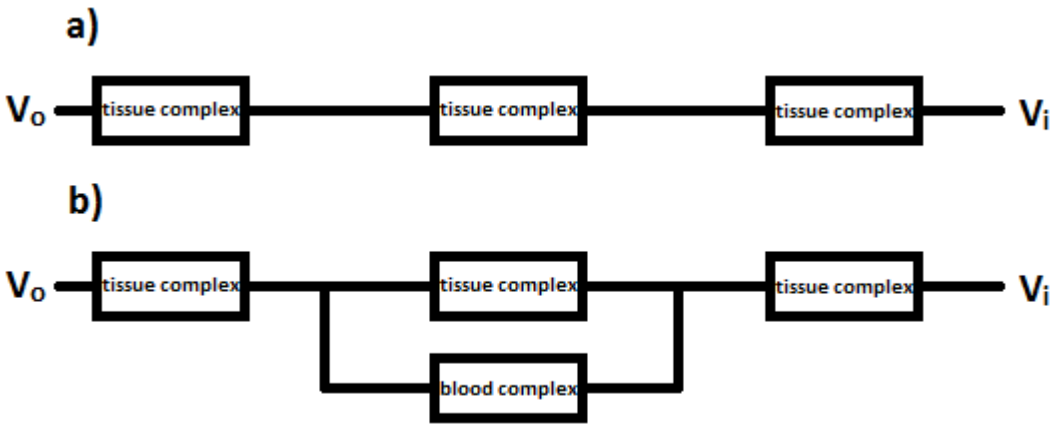

Figure 10 Circuit model of a) before the blood pooling occurs with the series of tissue complexes (combinations of different tissues ie. muscle tissue and fat), and b) when blood pools and provides a parallel path for the current at lower impedance.

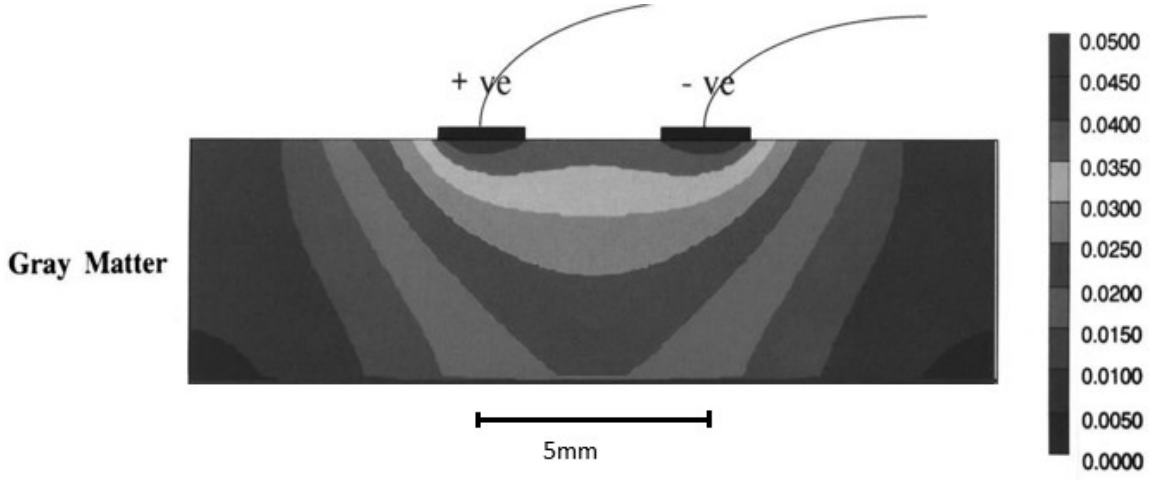

Figure 11 The current densities as depths, values are current densities (A/cm2). Modified from [12].

The depth explored by the applied current is determined by the electrical resistivity of the explored volume, the distance between the electrodes and the strength of the applied current. A study looking at depth explored, using finite element modelling of gray matter, found that the depth explored was equal to half the distance of the electrodes [12]. Gray matter is an appropriate approximation of the abdominal tissue since it is heterogeneous biological tissue with a similar resistance to abdominal tissue, with gray matter at 250 Ω·cm [12] and the abdomen at 500 Ω·cm [20]. At a depth of half the length, 2.5 mm in Figure 11, the current density is around 0.03 which is 60% of the input current density. Changes in this layer would still show a marked change in the measured value.

The lowered resistivity of blood compared to tissue, and the approximate depth explored in the abdominal cavity will be used to determine if internal bleeding is present and where it is present in the abdomen.

3.1.4 Prior Research in Internal Bleeding Detection

In 1992, Sadlier *et al.* at the University of Western Australia published results using electrical bioimpedance imaging which show considerable accuracy using a saline phantom. This group found that as little as 25 ml of blood could be detected within a mock saline abdomen using their impedance technique [7]. Their technique used a 16 electrode electrical impedance system with one input varying from 5 to 78 kHz.

Their phantom, a saline solution, was used to mimic the resistance of tissue at 5 Ω·m while four separate anomalies (saline and gelatin spheres, 1.5 Ω·m) were placed within the solution to represent the pooling of blood of different volumes. It should be noted that their solution was uniform aside from the blood volumes, and that there is no reference to their external resistance which models the skin. The volumes also did not change in size, so this experiment was solely examining if their system could detect and quantify the amount of blood present.

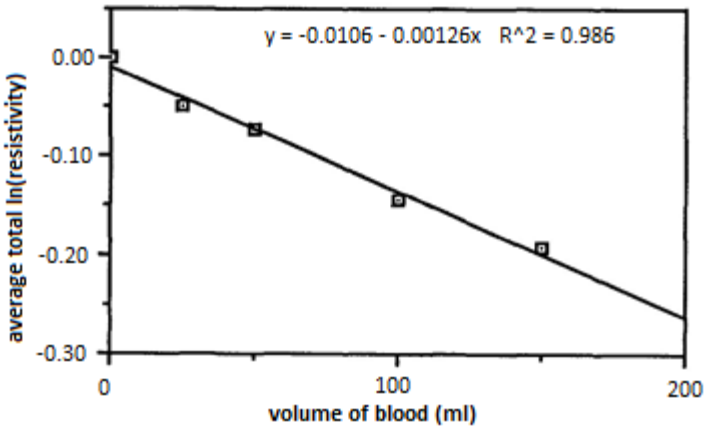

Figure 12 Total log resistivity change as a function of blood pool phantom volume. The data points represent 25, 50, 100 and 200 ml of blood pooled. Reproduced from [7].

It was found that the resistivity decrease when the volume of the blood pool phantom increase as shown figure 12. Although the experiments presented were lacking some necessary variability and data, the noticeable drop in resistance surrounding the pooled blood serves as proof of concept that the method of electrical bioimpedance should be able to detect the presence of blood at frequencies between 5 and 78 kHz.

More recent research has been done using pigs as a phantom for the human abdomen. Krantz *et al.* in 2000 [8] and Wanjun *et al.* in 2008 [9] both used pigs with EIT to detect bleeding with an accuracy of 30 ml. Krantz *et al.* calculated the volume of blood injected into each pig based on the weight of each. A value of 24 ml/kg was used and this amount was removed from each pig, then injected abdominally. Before being injected a small amount of saline solution was added to increase the total volume injected to 28 ml/kg. The pigs had a median weight of 30 kg, which gives a total volume injected at around 840 ml. Three pairs of electrodes were placed over each pig to give the impedance reading, and frequencies of 2.5 and 90 kHz were used. These electrodes were placed over the right sternocleidomastoid muscle, the left midaxillary line between the axilla and 12^{th} rib, and over the greater left trochanter. Results for 10 pigs are reproduced in Figure 13.

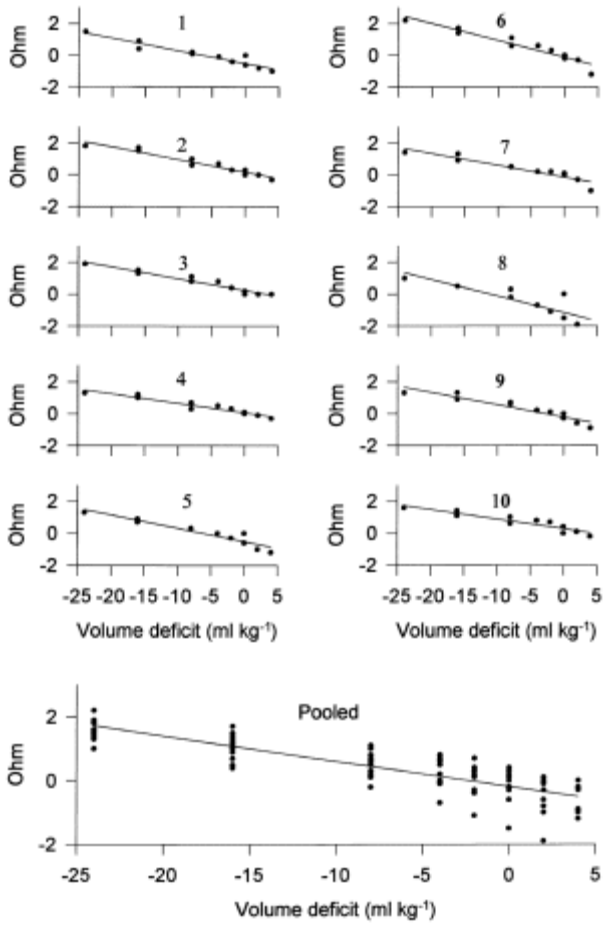

Figure 13 Linear resistance drops across the abdomen at 2.5 kHz related to the volume deficit in 10 pigs. Reproduced from [8].

The results in Figure 13 show a linear decrease of resistance with injected blood. This linear drop was seen across all 10 pigs. The amount injected, 28 ml/kg, would correspond to a value of approximately 2 l in an adult of 75 kg. Although this is a large amount of blood injected, a drop was noticed after 8 ml/kg, which would be roughly 600 ml in an adult of the same size.

Wanjun *et al.* injected blood into the peritoneum of pigs, at a steady rate of 100 ml/h. The volume injected ranged from 300-500 ml, at an average of 18 ml/kg. The bleeding was detected using a 16

electrode belt around the abdomen. The abdominal belt of electrodes allowed the creation of a 2D image to show the bleeding, as shown in Figure 14.

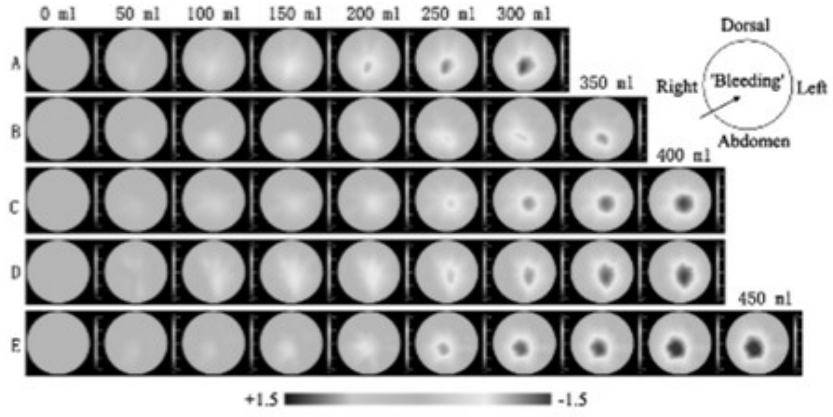

Figure 14 Reconstructed images showing the progression of the bleeding, reproduced from [9]. The images show abdominal cross-sections of 5 pigs (A, B, C, D and E) taken at 50 ml of injected blood intervals.

The Figure 14 clearly shows the presence of blood pooling within the peritoneal cavity. This blood begins to appear after 100 ml, seen in all 5 pigs in Figure 14. Using 50 kHz, Wanjun *et al.* demonstrated that their electrode belt was capable of detecting and locating bleeding found within the peritoneum of a pig.

At a conference in 2009, *Blumrosen et al.* [10] presented a full design for a continuous wearable internal bleeding detection method. Their method used varying frequencies employing magnetic induction coils. The justification for Magnetic Induction Tomography (MIT), over EIT was that MIT sensors could be contactless, making for quicker detection of bleeding. However, MIT loses the capability to locate the bleeding since it looks at bulk tissue changes solely. Although they achieved sensitivity of 20 ml, looking at a phantom of the human head, MIT is not a viable option since it lacks the ability to locate the bleeding.

3.1.5 Conclusion of Literature Review

The prior research presented shows a relationship between blood pooling and a decrease in electrical resistance. The goal of the research is to record this decrease in electrical resistivity and use an array of electrodes to locate the pooling. We hypothesize that the Z-Metrix will be able to detect the bleeding and a custom electrode array will be able to locate the blood pooling.

The design being presented will be based on the methods of *Sadlier et al.* and *Krantz et al*. The low frequency employed by *Sadlier et al.* of 5 kHz, the volume and flow rate per kilogram and high frequency from *Krantz et al.* will be tested.

In this work an electrode array to inject and read the current will be designed and fabricated for the experiments. This array will allow for rapid detection and localization of the bleeding. A certified medical device, *Z-Metrix,* to generate and process the signal will be used. Lastly, the data post-processing of a localization graphic for simple visual confirmation of the location of the pooling will be built. These three elements will provide a unique experimentation method.

3.2 Materials and Methods

3.2.1 Materials

All experiments are being performed using a function generator and receiver from BioParHom (*Z-Matrix*). The function generator has 2 output cables to close the circuit and 2 leads to measure the signals. These 4 cables are connected to a custom built multiplexer (built using an *Arduino Mega PIC*) which turns the 4 connections into 64 pin outs. The 64 pin outs are connected to a custom designed and built 8x8 needle electrode array, shown in Figure 15. The electrodes are made of stainless steel and are spaced 3.6 mm apart (for a total of 2.5 cm x 2.5 cm). All functions are run through a computer connected by USB to the function generator. Using *ZFlow* by Bioparhom, the function generator is controlled to run at set signal frequencies and durations.

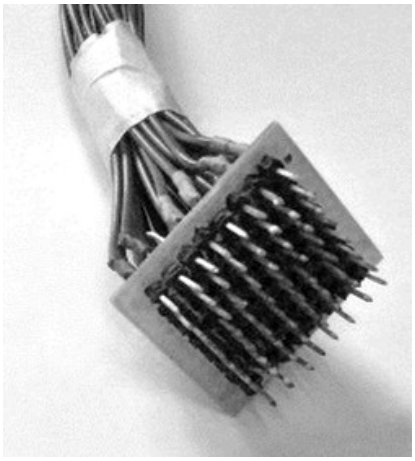

Figure 15 8x8 needle electrode array.

The function generator and multiplexer allow the signal to move position on the electrode array. Using this, 8 different current paths are chosen and inputted into the function generator. During the course of the 3 minute experiment, the signal changes which electrodes it closes the circuit with and which

electrodes act as leads each measurement. Sampling at 5-7 data points per second, in under 2 seconds every channel will have 1 measurement.

The phantoms are deceased female rats (*Rattus Norvegicus*) ranging in weight from 350 g to 500 g. The blood being injected is from American Yorkshire pigs, anticoagulated with Ethylenediaminetetraacetic acid (EDTA) at 2 mg/ml of porcine blood in diluted water at 8 ml/l of porcine blood.

The blood is injected through an 18 gauge stainless steel needle. The needle is connected to a 20 ml syringe (*BD Plastics*) via appropriate tubing, and is pumped at a constant rate of 10 ml/3 min using a syringe pump (*Nexus 3000* by *Chemyx Inc.*).

The tips of the needle electrode array are dipped in an EEG gel before being applied to the rat, ensuring that the gel does not short any connection between the needle electrodes. A custom suspension apparatus was built to allow the rat to rest on the needle electrode array (Figure 16).

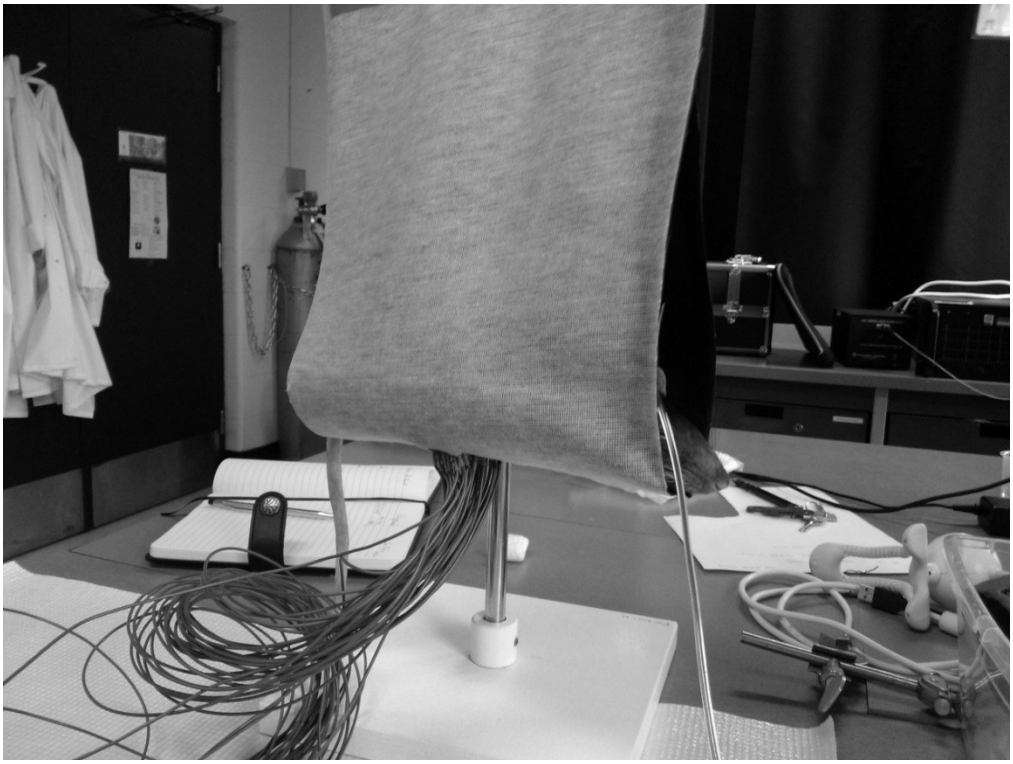

Figure 16 The experimental set-up showing the rat hanging in a 'hammock' to allow for easy placement of the needle electrode array.

3.2.2 Methods

Initially, the phantoms and blood are both brought to room temperature (20^0C). The abdomen of the rat is shaved exposing a 2.5 cm by 2.5 cm on the ventral side of the abdomen situated in the middle. The rat is weighed, if the rat is below 350 g, above 500 g or exhibits any severe deformities or alterations, it is omitted from the trial.

The function generator is attached to the multiplexer by the 4 cables, and also attached to the computer. *ZFlow* is run and the weight of the rat is inputted. In the software, the test frequency is specified (5 kHz, 95 kHz or spectroscopy depending on the experiment being run), and the duration is set at 180 seconds.

The electrode array is attached to the multiplexer through custom pin outs. The electrode array needles are tipped with EEG gel to ensure a thin coating. The needle electrode array is placed in the custom suspension apparatus to ensure the needles face upwards. The rat is rested ventrally on the needle electrode array with the shaved area matching the needle electrode array placement, seen in Figure 17.

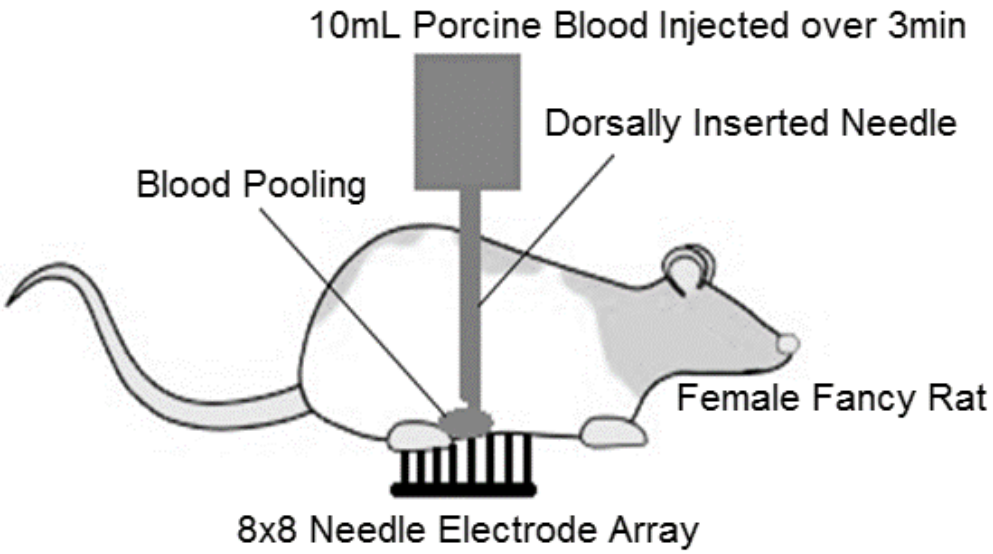

Figure 17 Schematic showing the location of electrode array, blood pooling and the syringe.

The blood is agitated gently for 10 seconds to suspend the RBCs. 10 ml of blood is entered into the syringe, and the syringe is attached to the 18 gauge needle via tubing. The syringe is placed into the syringe pump, and based on the size of the syringe an appropriate rate is selected to output 10 ml in 3 minutes (3.33 ml/min).

The 18 gauge needle is inserted dorsally into the rat and guide over the center of the needle electrode array until it is approximately 0.5 cm from the ventral skin. The needle may need support to maintain its position for the experiment.

The software and the syringe pump are run simultaneously to allow the 3 minute tests to match. Results of the test are stored within the software.

3.2.3 Experimental Trials

Table 2 provides a summary of all the internal bleeding experiments run, the rat and blood sample used, and the experiments results considered in this study are presented the by bold values. The measured weight if the rat and the frequency used is also represented.

Table 2 Summary of all rats, blood samples and experiments. Bold values are those whose results are presented.

Rat #	Weight (g)	Frequency (kHz)	Comments
1	367	5	Early proof of concept with early electrode grid
2	347	5	
3	341	5	
4	**360**	**5**	
5	**245**	**5**	
6	**395**	**5**	**Inflammation noticed near abdomen**
7	**345**	**5**	
8	400	5	Found short in wiring after experiments, data was rejected
9	353	5	

10	450	5	
11	410	5	
12	**326**	**5**	
13	**324**	**5**	
14	**296**	**5**	
15	**375**	**5**	
16	315	95	Early 95 kHz experiment
17	500	n/a	Rat was never tested
18	**450**	**95**	
19	**420**	**95**	
20	**440**	**95**	
21	**395**	**95**	
22	**350**	**95**	
23	**360**	**95**	
24	**440**	**95**	
25	**475**	**95**	
26	**430**	**95**	
27	300	spectrum	
28	285	spectrum	
29	285	95	Early 95 kHz experiment

3.2.4 Statistical Analysis

For the analysis of the data for internal bleeding, several statistical tools are used. Since we are hypothesizing that as the blood pools, electrical bioimpedance will detect a change in resistance across the abdomen, a correlation is required to show that the data for resistance measured exhibits a change with time. To do this, linear regression, correlation of determination and significance from a 1-tailed t test are used.

Linear regression attempts to follow the data points from a current path with a line. The purpose of the regression line is to give a slope value from the data points which we hypothesize is correlated to the rate of bleeding along a current path. This correlation significance is discussed in section 3.4. Figure 18 shows the regression line and its representation of the data general downward slope.

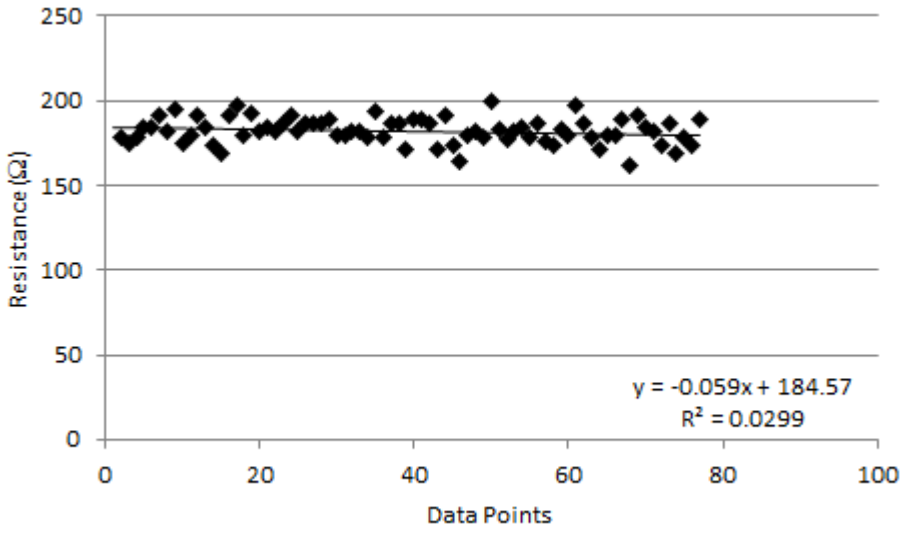

Figure 18 Sample data showing the data points and the trendline, from Rat 5.

The correlation of determination (R^2) represents the percentage of the data that can be described by the linear trend between x and y.

$$R^2 = \left[\frac{N\sum xy - (\sum x)(\sum y)}{\sqrt{N\sum(x^2) - (\sum x)^2} + \sqrt{N\sum(y^2) - (\sum y)^2}}\right]^2$$ *Equation 1*

For Equation 1, x represents the time, and y represents the resistance value. n is the number of data points (close to 80). The t value is the value for a Pearson correlation test. An R^2 value of 1 shows strong correlation, while a value of 0 shows no correlation. The correlation of determination has limitations for horizontal lines. Slopes with horizontal lines do not give a correlation. Even though the best fit line works well, the R^2 value approaches 0. For this research, an R^2 value of 0 could mean that there is no variation in the impedance, so no blood pooling.

To account for the high number of data points, the significance value was found from a one-tailed t-test. The test is one tailed since only negative slopes hold significance because a drop in impedance should correlate to an increase in blood volume over the current path.

$$t = \sqrt{\frac{R^2(n-2)}{1-R^2}}$$ *Equation 2*

With this t value, a significance (p-value) can be found [21], described in Table 3.

Table 3 One-tailed significance (p-value) for a t-value with a sample size (n) [21].

	One-tailed significance (p)				
n	.05	.025	.01	.005	.0005
5	.80	.88	.93	.96	.99
6	.73	.81	.88	.92	.97
7	.67	.75	.83	.87	.95
8	.62	.71	.79	.83	.93
9	.58	.67	.75	.80	.90
10	.55	.63	.71	.77	.87
30	.31	.36	.42	.46	.57
40	.26	.31	.37	.40	.50
50	.23	.28	.33	.36	.45
60	.21	.25	.30	.33	.41
80	.19	.22	.26	.29	.36
100	.17	.20	.23	.26	.32

From the p-value table, using an n of 80, with a t-value of less than 0.26, we achieve a significance of $p<0.01$. For this work, a $p<0.1$ will be marked as *, $p<0.05$ will be marked as ** and $p<0.01$ will be marked as ***.

To justify the use of Gaussian statistics, the data measured must exhibit Gaussian distribution. To test this, the data for current paths affected by bleeding is combined and distributed in Figure 19 and the current paths that do not cross the bleeding are combined in and distributed Figure 20.

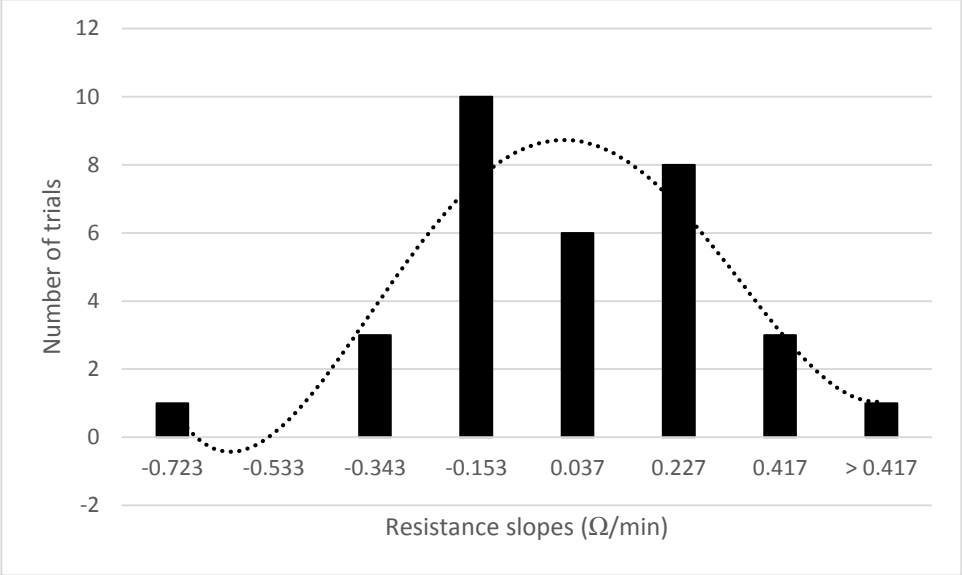

Figure 19 Distribution of data around the bleeding at 5 kHz.

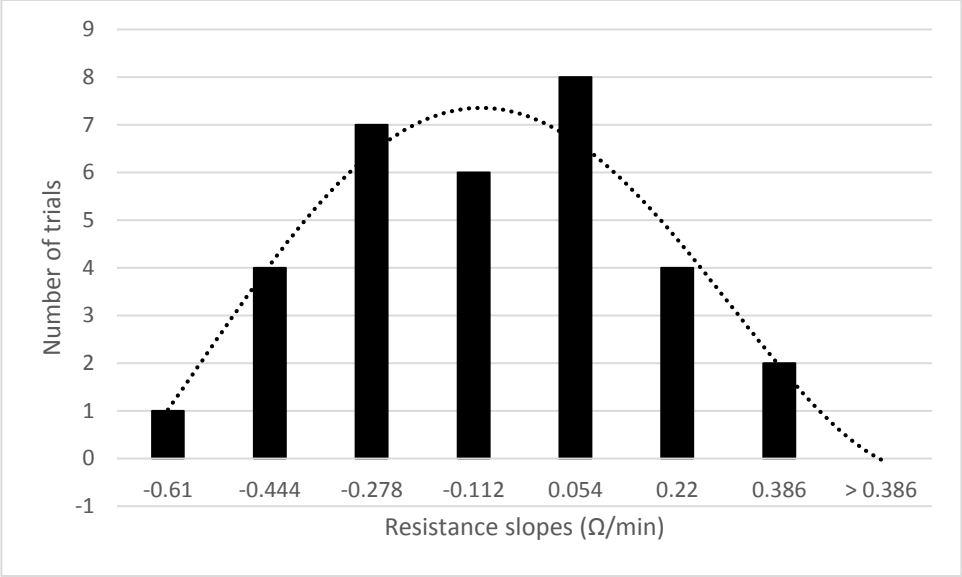

Figure 20 Distribution of data through the bleeding at 5 kHz.

Since plots show Gaussian distribution in the data, Gaussian statistics are deemed appropriate for the statistical analysis.

To represent all the data in an efficient manner and eliminate the effects of outliers, box and whisker plots were used. These utilize the median, 25th percentile and 75th percentile. As well, box and whisker plots use the furthest point within 1.5 times the gap between the 25th and 75th percentile as the outlier, shown in Figure 21.

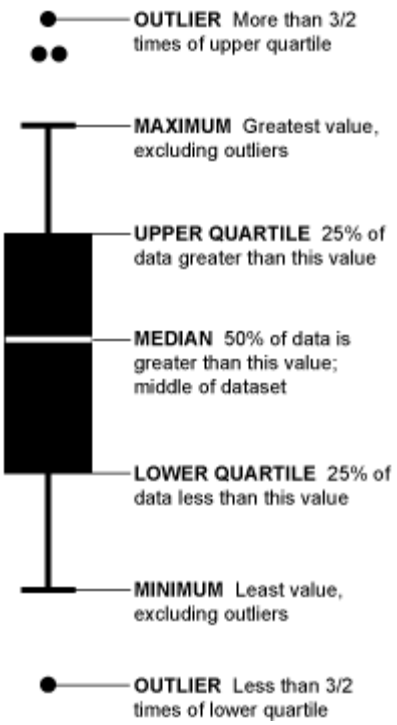

Figure 21 Graphic explaining the components of a box and whisker plot [22].

3.3 Results and Discussion

3.3.1 Internal Bleeding Detection

Internal bleeding detection was done using a 3 minute time frame taking measurements at a constant frequency. 5 kHz and 95 kHz were used in different experiments to compare their sensitivity to blood pooling. A decrease in resistance over the 3 minutes signified a change across a current path, and for these experiments symbolized blood pooling. This relationship is isolated during these experiments because is performed on deceased rats, and the only change being measured is the pooling blood.

A sample of data can be seen below for results at 5 kHz. What is shown is that the linear trend is either negative (Figure 22) or positive (Figure 23) depending on if there is or is not blood pooling respectively (verified visually after the completion of the experiment).

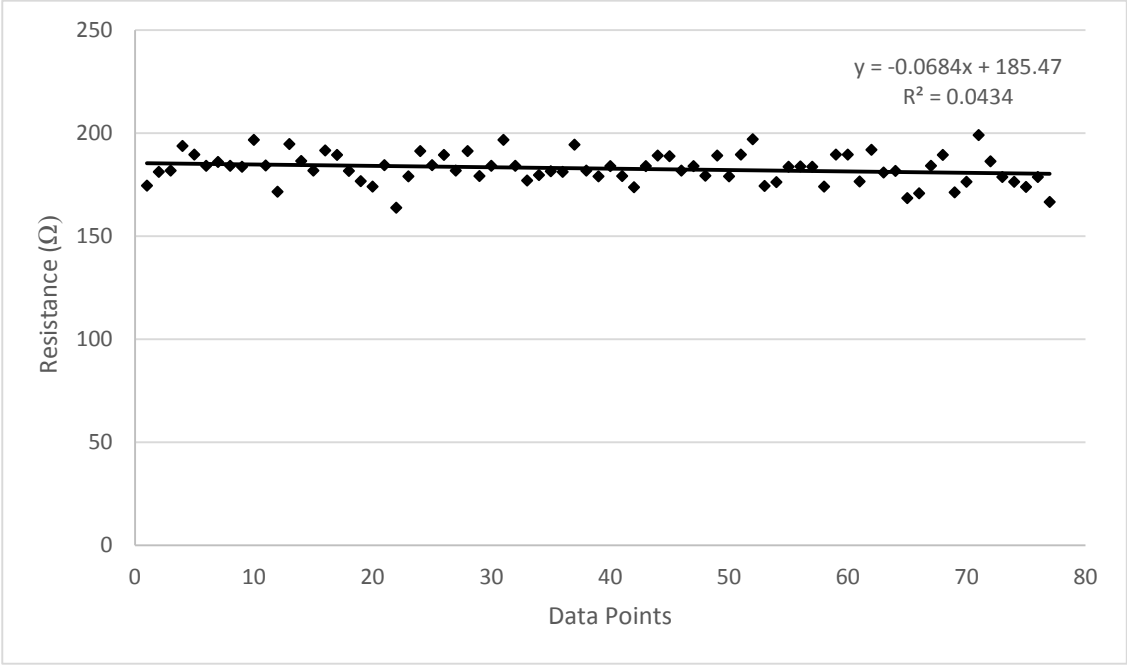

Figure 22 Graph showing sample data of changes in resistance over current paths going through the blood pooling at 5 kHz from Rat 5.

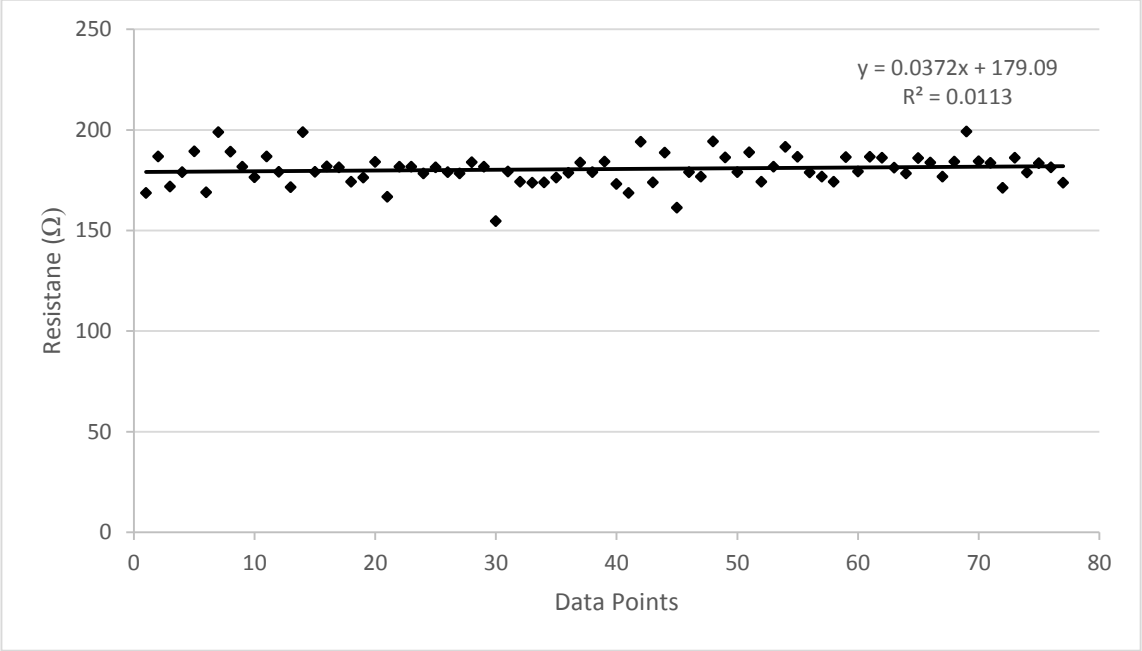

Figure 23 Graph showing sample data of changes in resistance over current paths going around the blood pooling at 5 kHz from Rat 5.

What is also seen is that there is noise in the signal. Over the 3 minutes (approximately 80 data points), the signal oscillates (at either 5 kHz or 95 kHz), which makes achieving a high correlation value difficult. This oscillation makes the value of the trend noise dependent since noise in the measured values will have a large effect on the slope. A time frame to measure the slope of less than 3 minutes is advantageous, since it will create faster detection, it can add error to the noise. For consistency, all the measurements and localization occurred over 3 minute timespans.

With the theoretical position of blood pooling in the center of the array, we expect the 4 paths that cross the bleeding should show a drop in resistance due to the presence of blood. Plotting the average slope values for all the experiments, we obtain a graph of all the changes over the whole time. A sample of this is shown for 5 kHz in Figure 24.

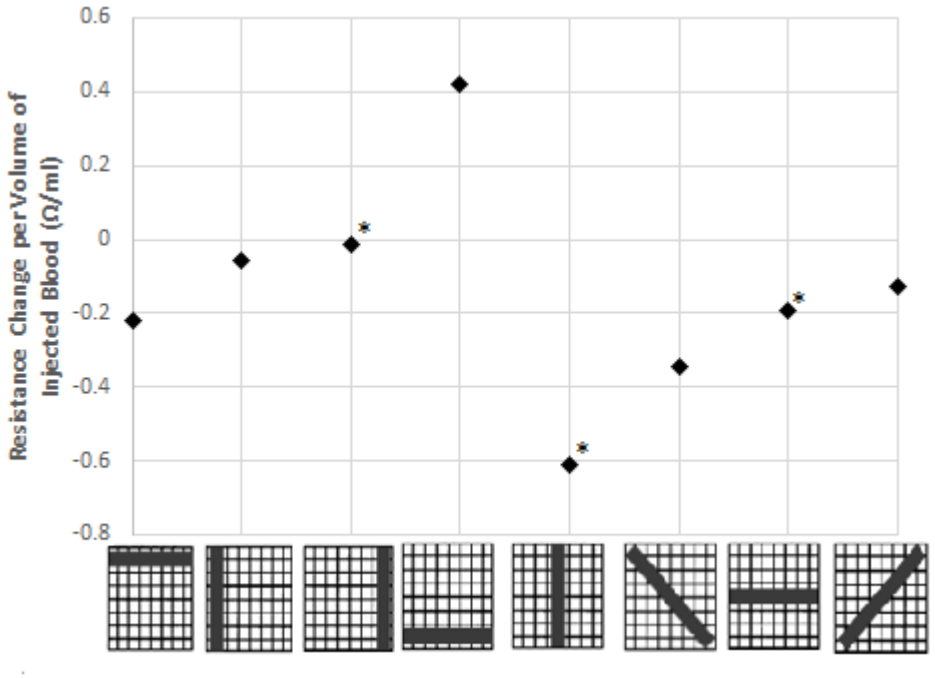

*Figure 24 Sample showing the resistance change per ml of injected blood (the slope of the line for each channel over the 3 minutes). * represents the significance (p-value). Sample was taken at 5 kHz with Rat 6.*

From Figure 24, we can see that the areas where the bleeding is expected, due to the placement of the needle injecting the blood (the last 4 current paths), show the greatest drop in resistance. In this sample, the 4th data point shows a marked increase in resistance, this is assumed to be due to the pressure of the pooling blood. The additional blood may have moved tissue with a high resistance into the 4th current path, causing an increase in resistance.

Combining the data for all the rats at 5 (Figure 25) and 95 (Figure 26) kHz creates the following graphs.

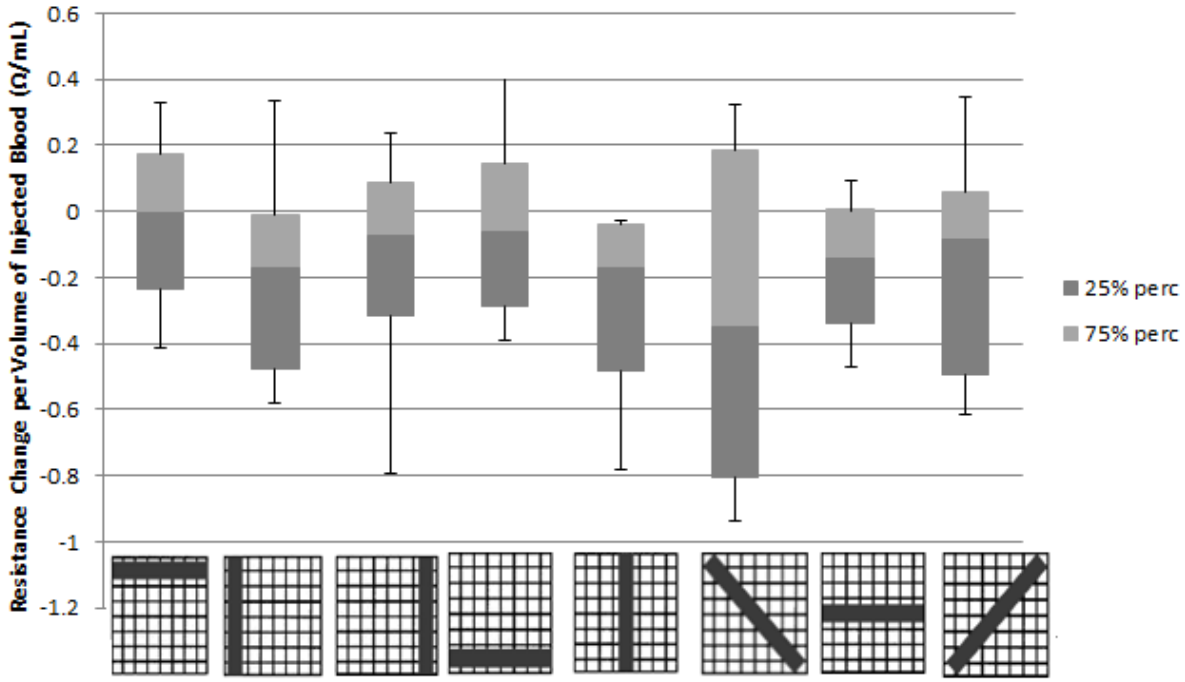

Figure 25 The box and whisker plots for the results of all the experiments at 5 kHz, showing the average resistance changes for a given current path. N=8.

This displayed a high level of variability between the experiments. An explanation for this variability is that the pooling did not always occur directly in the middle, and it did not stay directly in the middle of the array. This will be investigated more in section 3.3.2. This spread would cause drops in resistance along paths which would otherwise be unaffected. As a result a large, and predominately negative, range of values was seen in Figure 25.

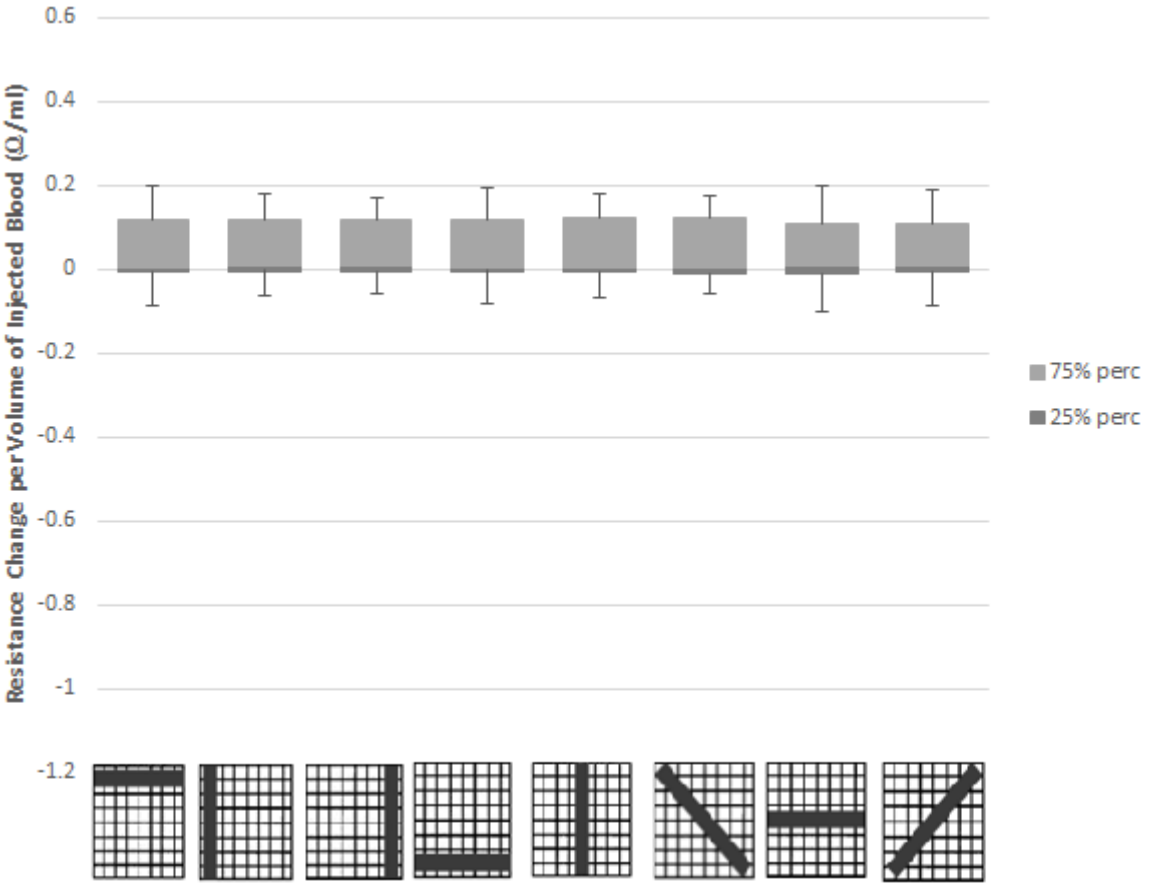

Figure 26 The resistance change per volume of injected blood of all the experiments at 95 kHz, showing the average resistance changes for a given current path. N=9.

Figure 26 shows the resistance change per volume of injected blood at 95 kHz. What is noticed is that there is almost no variability between current paths. A possible explanation is that at 95 kHz, the tissue impedance is low enough that the addition of the blood does not significantly alter the measured resistance. The drop in tissue impedance can be seen in the compendium by *Geddes* and *Baker* [16], where muscle tissue in a guinea pig changes its resistivity from 1840 Ω·cm at 1 kHz to 435 Ω·cm at 100 kHz. As a result of this low sensitivity, for the localization the 5 kHz frequency will be used.

For the resistance variations obtained at 5 kHz, the significance of the linear relationship (p-value) was calculated from the correlation values (R^2) as describe in 3.2.6. The plot in Figure 27 presents p-values for all of the individual experiments and the current paths.

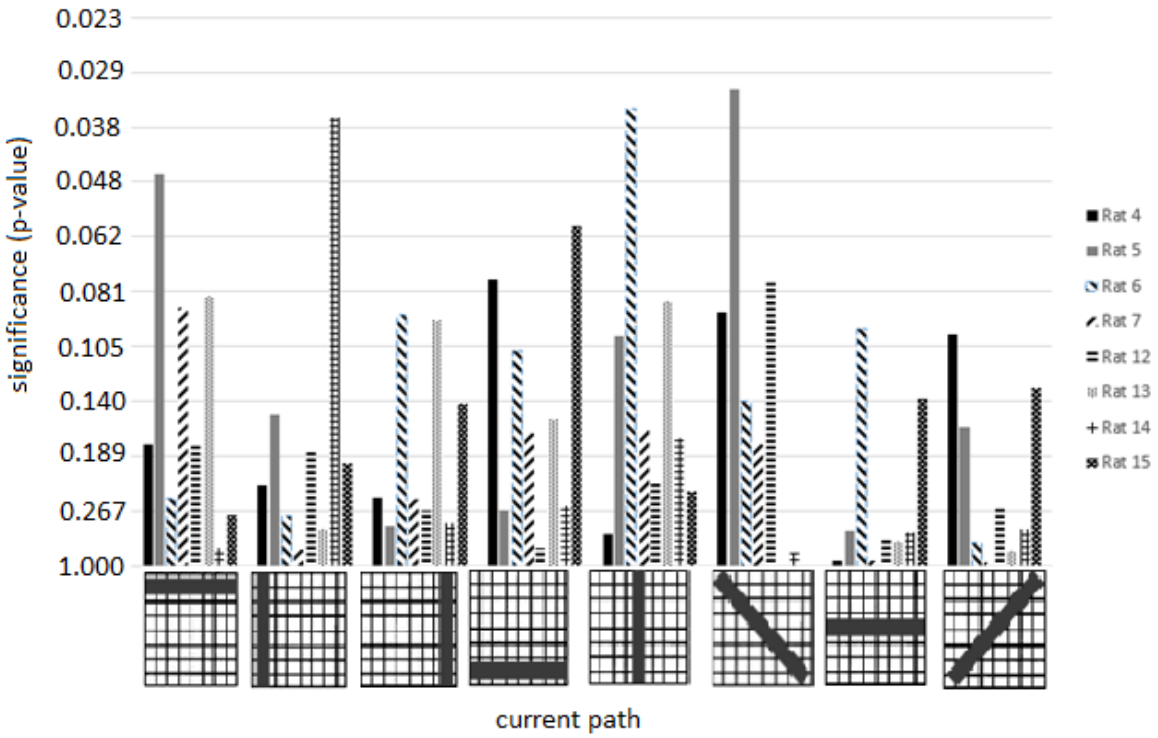

Figure 27 The significance (p-values) for the linear slopes along each current path for each rat at 5 kHz.

Due to the high variability within the individual signals, along with a high number of data points the correlation values were found low. This correlation is not enough to show a relationship between the measured data points and the linear trend lines used to show the presence of blood pooling. Using compensation for the high number of data points, the significance of the values are presenting figure 29 and in Table 4. 14 p-values were found below 10% significance.

*Table 4 The slope and significance values (1 tailed t-tests) for 8 rats at 5 kHz. * p<0.1, **p<0.05, ***p<0.01.*

	Slope (p value)							
Rats	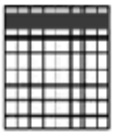	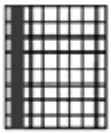	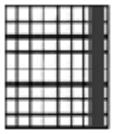	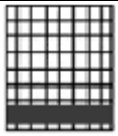	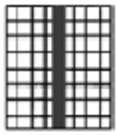	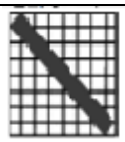	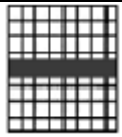	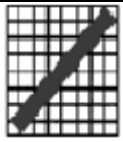
4	-0.166 (0.177)	-0.407 (0.225)	-0.270 (0.243)	-0.003* (0.076)	-0.101 (0.314)	-0.382* (0.089)	-0.327 (0.420)	0.182* (0.100)
5	-0.291** (0.047)	-0.354 (0.150)	0.178 (0.300)	0.215 (0.266)	-0.161* (0.100)	0.348** (0.032)	0.094 (0.310)	-0.585 (0.159)
6	-0.217 (0.250)	-0.058 (0.274)	-0.012* (0.091)	0.418 (0.110)	-0.610** (0.035)	-0.125 (0.139)	-0.191* (0.097)	-0.346 (0.339)
7	0.329* (0.088)	-0.121 (0.370)	-0.234 (0.246)	-0.321 (0.166)	-0.317 (0.161)	-0.050 (0.177)	0.011 (0.420)	-0.360 (0.441)
12	0.163 (0.177)	0.332 (0.182)	0.237 (0.266)	-0.123 (0.359)	-0.312 (0.221)	0.216* (0.077)	-0.168 (0.323)	-0.536 (0.260)
13	0.170* (0.082)	0.127 (0.305)	-0.132* (0.092)	-0.327 (0.155)	-0.030* (0.085)	-0.467 (0.493)	-0.116 (0.339)	-0.424 (0.376)
14	0.163 (0.362)	0.332** (0.036)	0.237 (0.289)	-0.123 (0.254)	-0.312 (0.170)	0.216 (0.379)	-0.168 (0.314)	-0.536 (0.305)
15	-0.413 (0.272)	-0.286 (0.196)	-0.723 (0.142)	-0.190 (0.059)	-0.041 (0.232)	-0.528 (0.493)	-0.219 (0.137)	0.326 (0.131)

For internal bleeding detection, a low frequency of 5 kHz was able to detect the presence of blood. 95 kHz proved to have a low sensitivity to blood pooling.

3.3.2 Bleeding Localization

The localization of the internal bleeding is as important as the detection itself. In order to locate the bleeding, the slopes along each current path were compared. Using data from graphs such as Figure 24, an image of where the bleeding is occurring begins to form.

The method works by dividing the area encompassed by the electrode array into a 3 by 3 localization grid. Each electrode path on the 8x8 array crosses through 3 of the squares in the localization grid. For example, in the top left sector of the 3x3 localization grid, highlighted in Figure 28, 3 current paths affect the value in that corner because they cross through the sector, shown on the right of Figure 28. Averaging those 3 current paths slope value, we achieve a value for the segment of the localization grid

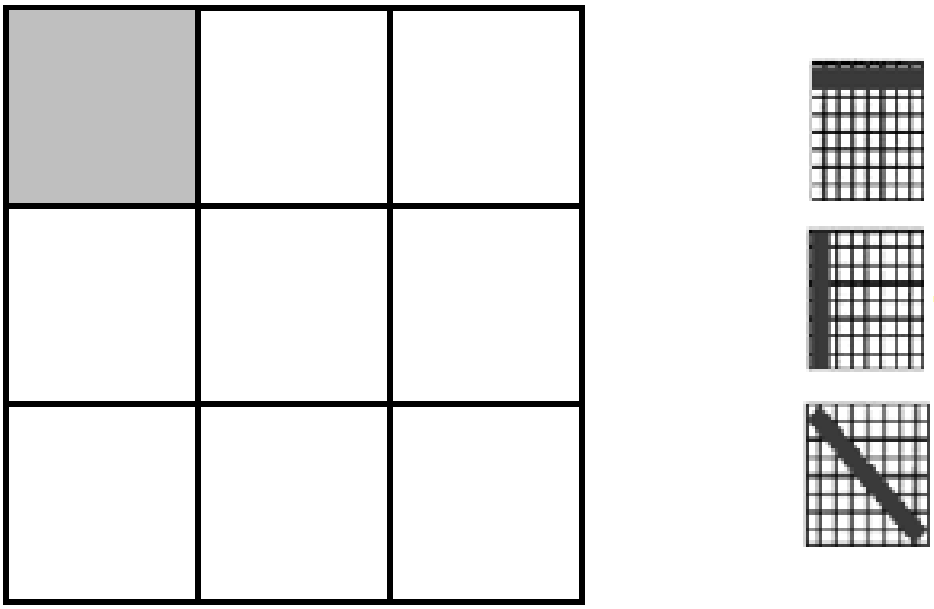

Figure 28 Schematic of 3x3 localization grid showing the highlighted top left sector. The diagrams to the right show the 3 current paths which influence the highlighted sector of the grid.

Averaging the slope value of the resistance change for each electrode path within the square gives a picture of the impact the square had on the resistance drop value. Using this method as shown in Figure 29, an image begins to form of where the greatest change in resistance is occurring.

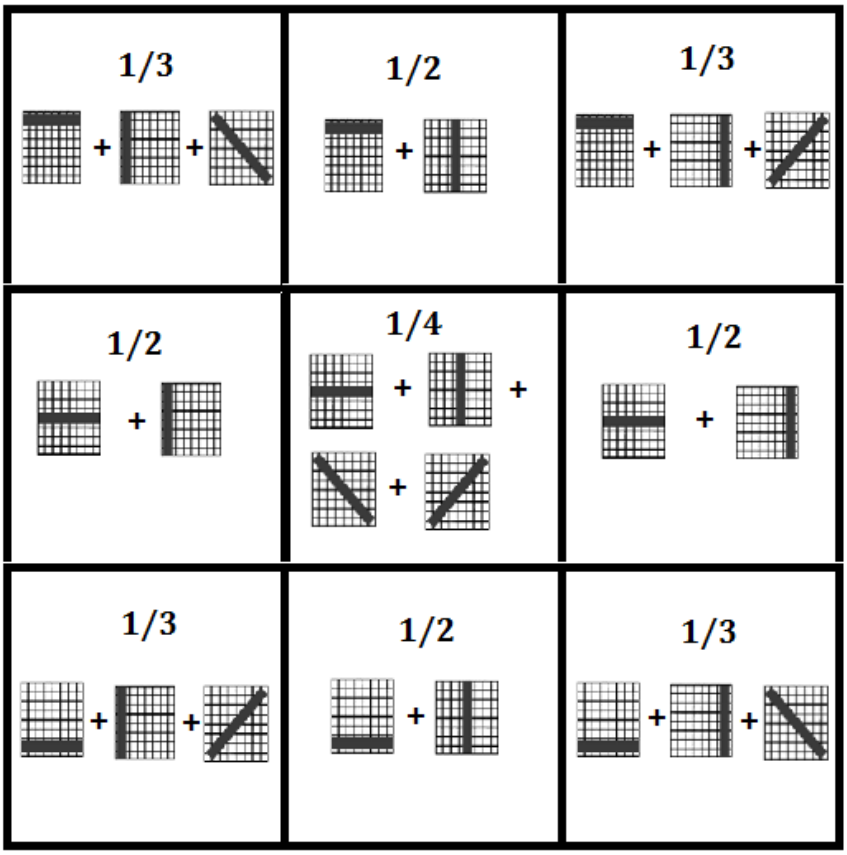

Figure 29 Schematic of how the localization occurs. The current path images represent the slope along that path.

A sample of the localization creates Table 5:

Table 5 Color coded grid showing the probable location of bleeding. The values are the averaged slopes at the location. The darker the color, the greater slope and more probably bleeding location. Taken from Rat 15.

-0.12	-0.27	-0.55
-0.25	-0.12	-0.47
-0.33	-0.12	-0.20

For several of the rats, bruising was visible after the experiment. These cases are presented below. The needle electrodes left an imprint on the skin, this allowed the bruising to be placed within the grid. Comparing the localization grids, shown in Table 5, to the visible bruising allows validating the method. The correspondence between the darker regions in the localization grids and the visualization of the bruising is shown Table 6.

Table 6 Comparisons of the bruising locations (outlined) with superimposed gridlines under Bruising and the measured Localization Grid at 5 kHz.

Rat	Bruising	Localization Grid
Rat 6	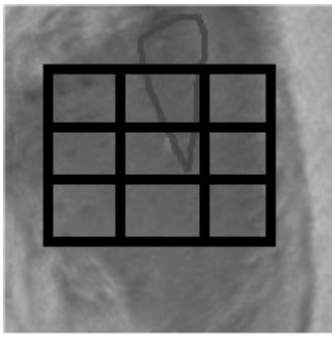	-0.21 -0.41 -0.12 -0.12 -0.32 -0.10 0.08 -0.10 0.02
Rat 14	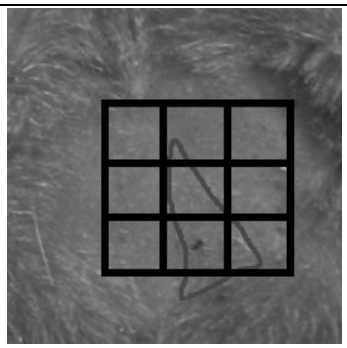	-0.01 -0.07 0.20 0.08 -0.20 0.03 0.14 -0.22 -0.14
Rat 15	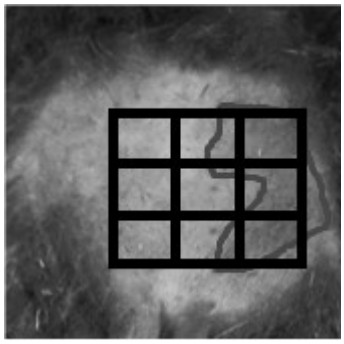	-0.12 -0.27 -0.55 -0.25 -0.12 -0.47 -0.33 -0.12 -0.20

The localization grids show strong correlation to the bruising locations when present, and provide early evidence of the set ups capability to detect and locate internal bleeding. For the experiments, a limited number of trials showed visual confirmation of the blood pooling location. A higher number of visual verifications would help verify and improve the localization process.

3.3.3 Discussion of Experiment Setup

3.3.3.1 Animal Model

For proof of concept experiments, a phantom has to be chosen to model a human subject. A model is used because the experiments are in early stages, so trials on human subjects would be premature without initially showing efficacy on a phantom. Fancy Rats (*Rattus Norvegicus*) were used.

For internal bleeding detection, the areas of interest for the phantom were its tissue impedance, its anatomy and its blood to tissue ratio.

The anatomy of the rat is favorable since it has a relatively large abdominal cavity, suitable for blood pooling. The size of the abdominal cavity allowed for adequate space to place the electrode array, insert the needle and inject the blood. This made for an easier set-up. With its size, it also allowed for increased depth, allowing the blood to pool deeper within the cavity and making more difficult trials for the detection.

The rat has the same blood to tissue ratio as a human being of 7% [23] [24]. This equivalent ratio allowed the effect of the added blood to be similar in the rat as it would be in a human. The rats had an average weight of about 380 grams, making them about 1/185 the weight of a 70 kilogram person.

We should note that rat abdominal tissue has a resistivity of 150 Ω·cm [25], while human abdominal tissue is around 500 Ω·cm [20].

For all the experiments impedance change as a result of blood volume changes was the measured value. As a result, the quality of the experiments relied heavily on the appropriate blood used. The experiments performed were early stage proof of concepts, so human blood was not used. Porcine blood, from the American Yorkshire pig (*Sus Scrofa Domesticus*) was used in place of human blood in all experiments.

3.3.3.2 Design of Electrode Grid and Current Paths

The goal of the set-up is to detect and locate the internal bleeding. Due to the need for location, a grid or pattern must be used to determine where the bleeding might be.

Electrical Impedance Tomography (EIT) is a method commonly used for creating a 2D image of a cross-section using impedance, allowing for location of blood pooling to be seen. EIT is an effective tool for imaging, however it was not considered for this research. The main reason was the device used in the experiments, *BioParHom Z-Matrix*, does not support EIT measurements. Other concerns with EIT are that it would not be a viable alternative for internal bleeding detection since it is intensive to set up, requiring a belt of electrodes to surround the desired cross-section on the patient. As well, if the placement is off, it requires more work to relocate the belt. For these reasons, EIT is not a viable possibility for rapid detection of internal bleeding.

An 8 by 8 needle electrode array was designed and fabricated to allow for the localization to occur underneath it, as shown in Figure 30. Its dimensions, adapted to the size of a rat, are 2.5 cm by 2.5 cm, with a spacing of 3.6 mm between each electrode. This size equated to covering approximately 80% of the rats abdominal cavity. The electrode material is stainless steel. This design, although adequate for proof of concept experiments would not be allowed for human trials. The needle electrodes would have to be changed to reduce risk to the patient. As well, covering 80% of the abdomen is a large area. Designing a smaller patch would be beneficial, however the effects would have to be investigated.

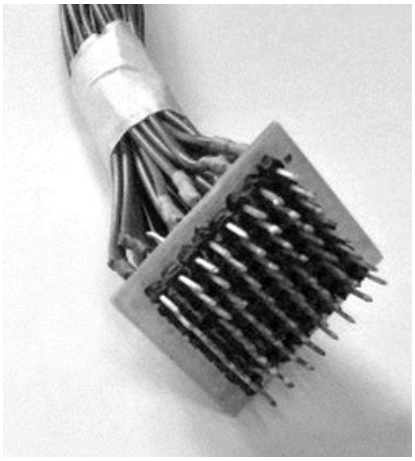

Figure 30 8x8 needle electrode array.

The noise created by the electrode array was not analyzed. Experiments on phantoms, and with limited components to isolate sources of noises would have the possibility to improve experimental results and the design as a whole.

With the electrode array, a localization pattern needed to be used to identify where the bleeding was occurring. The function generator (Z-Metrix) was attached to an Arduino powered multiplexer, which put the current through different paths on the array, creating the localization pattern seen in Figure 31.

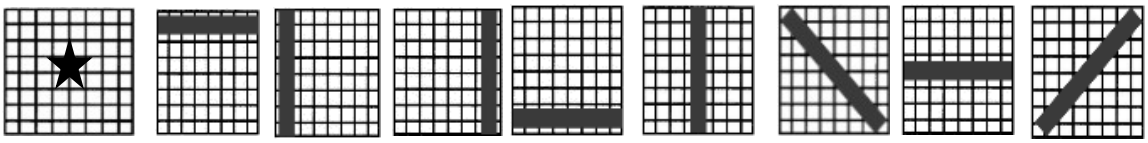

Figure 31 Schematic showing the location of the blood pooling as a star on the electrode array as well as the 8 different current paths.

With a sampling rate of 5-7 data points per second, the function generator (*Z-Metrix*) and multiplexer runs current through 1 current path at a time. This gives each current path about 1 measurement every 2 seconds.

To make the current path, a 4 electrode configuration is used, as was discussed in section 2.3. In order to maintain this, the grid must utilize current injection electrodes and leads placed accordingly. Both injection electrodes and leads must change positions for each measurement to ensure the measured volume is placed between the injection electrodes, shown by the lines in Figure 31. One note is that the 4 electrode configuration measures mostly between the leads (which are placed between the injection electrodes), this makes the measured area smaller than the overall electrode array area.

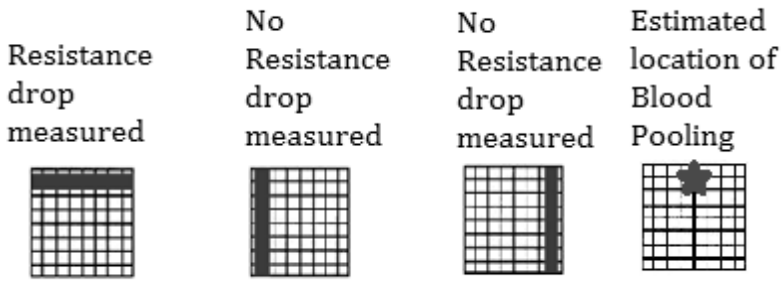

Figure 32 Schematic showing how the localization process works with the alternating current paths.

Figure 32 shows a sample case for the localization of the blood pooling. Averaging the current path across sections of the array it crosses, we get a value which approximates the impact the blood pooling has on that particular section of the array. Using the estimation process outlined in Figure 32, we expect the 8x8 needle electrode array to be able to localize any blood pooling being detected.

We hypothesize that utilizing this electrode configuration, and the alternating pattern of the current injection, localization can occur.

3.3.3.3 Electrical Frequency

Biological tissue has a range of responses to electrical current which depend primarily on the frequency. As was shown in section 2.1, for the detection of internal blood pooling, a lower frequency was expected to be more sensitive to blood pooling since the low resistance value of the blood plasma had an increased effect. This was due to the added influence of the plasma as a conductive fluid, and would minimize any impact capacitance has on the output.

Shown in previous work, the chosen value range of the signal frequency was from one kHz to hundreds of kHz: *Krantz et al.* used 2.5 kHz (0.25 mA) and 90 kHz (1.5 mA) [8] for their experiments using pigs, *Wanjun et al.* used 50 kHz (1 mA) [9] for their experiments, also performed on pigs, *Sadlier et al.* used between 5 kHz and 78 kHz (no current stated) [7] for their experiments on a cylindrical saline phantom and 6 years later *Sadlier et al.* used between 5 kHz and 39 kHz (no current stated) [20] on saline filled PVC tubes. All the previous research shows that the frequency used stays below the threshold frequency required for current to enter into the cell, which is around 100-150 kHz [1].

For the experiments, a frequency of 5 kHz and 95 kHz were used to measure the resistance across the abdomen of the rat over 3 minutes of blood injection. This encompassed the range of frequencies used by previous research and would provide validation of the theory stated in section 2.1 pertaining to the sensitivity at lower frequencies. As well, impedance spectroscopy will be performed on two rats before and after bleeding to quantify the frequencies which are the most sensitive to the addition of blood. The results from the spectroscopy will be used to evaluate (improve) the frequencies chosen for these experiments, as well as those used in previous research.

3.4 Conclusion and Future Work

The work presented shows a correlation between the measured resistance drop across a path and the presence of blood pooling. The linear trends were not all found to be statistically significant as a representation of the resistance drop with time. The lower frequency used of 5 kHz was determined to be more sensitive to the presence of blood pooling, while the higher frequency of 95 kHz exhibited no change with blood pooling.

Using an original localization method, visual representations of the blood pooling location were created, and matched with those rats who displayed bruising. There was visual corroboration between the two.

Future work would look at improving and automating the visual localization plot. This would simplify the experiment. To improve the localization, refining the algorithm used could provide better insight into the bleeding location.

As well, a calibration factor to relate the resistance drop to the blood pooling rate would be created. With this factor, the localization plots could be compared to determine the severity of each case. This would require more testing with different volumes and rates being injected, and possibly several injection sites at one time.

In conclusion, the Z-Metrix was found to be capable of detecting internal bleeding, and the method created located the pooling on the electrode grid.

4 Erythrocytes Aggregation

Red blood cell (erythrocyte) aggregation is a physiological process where red blood cells (RBCs) form reversible aggregates in slow flows that usually take the form of a rouleaux or complex three-dimensional structures. When the flow rate is increased, shearing forces disaggregate the rouleaux, and the RBCs return to their individual state. Vice versa, at rest RBCs tend to aggregate. RBC aggregation is an important indicator for physicians for the health of the circulatory system. The current estimation method involve *in vitro* settling of blood as the greater the aggregate, the faster the settling, however it takes over 2 hours. The time required for the experiments warrants research into new method of study.

Utilizing electrical bioimpedance which is hypothesized to show a reactance change as the blood aggregates, and a similar index as is used for light transmittance measurements (AI) of aggregation index (AI_c), a method was developed using frequency to maximize the impact of reactance change in the blood. Using the *Z-Metrix* with a 4 electrode configuration to test 2 ml of porcine blood mixed with 2 mg/ml of EDTA for 2 minutes at a single frequency, the areas of the reactance vs time plots were used to calculate the AI_c. The 304 kHz was found to be the most sensitive of the frequencies tested to reactance changes during aggregation. Results found for blood samples gave an average AI_c of 27.32 ± 11.44, which was within the physiological range for porcine blood of 3-30. It was found that the 304 kHz had a higher precision than the 100 kHz frequency, but the AI_c were within the same magnitude. These early results show promise for the use of electrical bioimpedance as a rapid method for AI measurements.

4.1 Background

4.1.1 Aggregation

Blood aggregation is the natural and reversible stacking of red blood cells (RBCs). Aggregation is different from clotting because it is reversible. When aggregation occurs, blood cells stack face-to-face, similar to a roll of coins shown in Figure 33. These aggregates are weakly held together; as a result mild shear rates can break the bonds formed.

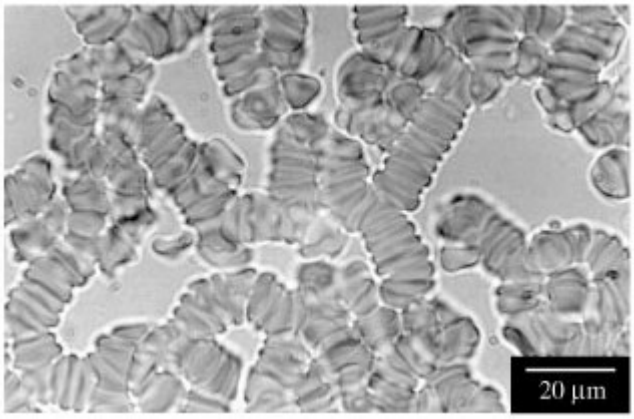

Figure 33 Example of blood aggregation, reproduced from [26].

Important medical assessments of blood aggregability are the sedimentation rate (the rate at which the red blood cells settle in static suspension) and the aggregation index (AI). The blood aggregability is used as a diagnostic tool for physicians as it is an indicator for several blood ailments, such as sepsis. For severe cases of sepsis, the mortality rate can increase by 7% per hour if antibiotics are delayed [27]. Due to this severity, a rapid and accurate detection of the AI is necessary.

There are many biological factors which influence blood aggregation, and all of its mechanisms are not fully understood [28]. Many factors such as blood cell structure, macromolecules and fibrinogen all affect red blood cell aggregation. This makes secondary measurements of blood aggregation difficult,

since it is dependent on more than 1 factor. This shows the need for a rapid and accurate device which directly measures blood aggregation.

4.1.2 Current Blood Aggregation Detection Methods

The clinical blood aggregation detection method is the sedimentation rate test. Blood aggregation creates large clusters of red blood cells that settle quicker in suspension than normal blood, as it change the balance between drag force, buoyant and gravity forces. There is a correlation between the settling of blood and the aggregation rate.

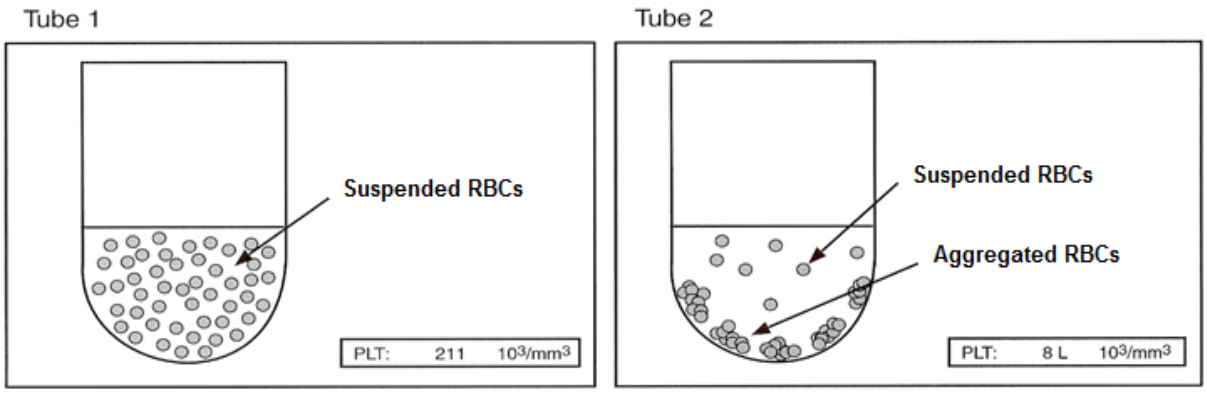

Figure 34 The relative impact of the RBCs on the cross-section comparing when fully suspended and when aggregated. Modified from [29].

Figure 34 shows the impact of blood aggregation on blood settling. The test has two drawbacks. The first is that the sedimentation rate experiments take an average of 2 hours to run [30]. This provides a long window before any treatment can be given to the patient. The second drawback is that the experiment is run *in vitro*, and the blood must be removed from the patient and tested elsewhere. This means all blood aggregation tests create discomfort for the patient and a delay in the static result of the aggregation index.

Light transmittance is an experimental method which passes light through the blood and measures the amount of light that makes it through the solution over time [28]. As more blood aggregates, more light passes through the blood, and the aggregation index goes up, displayed in Figure 35.

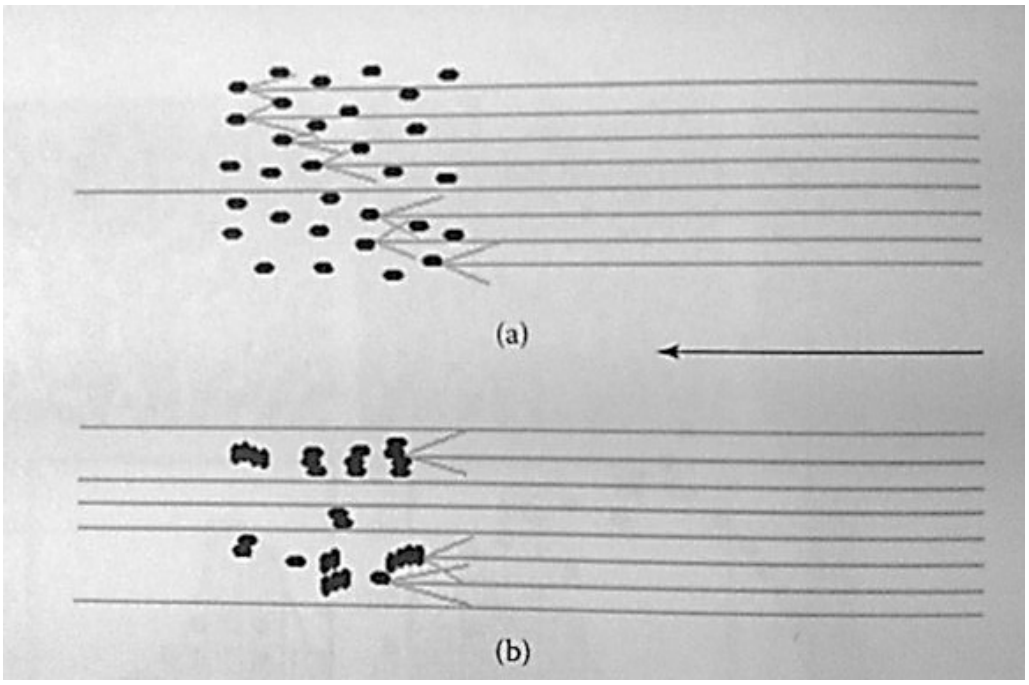

Figure 35 Light transmittance through a blood solution when a) the RBCs are still suspended and b) when the RBCs have aggregated. The increased light transmittance is clearly shown in the aggregated image [28].

To calculate the aggregation index, Light transmittance uses the following method, reproduced in Figure 36. This method takes the area above and below the curve, then finds what percentage of the total area is below the curve.

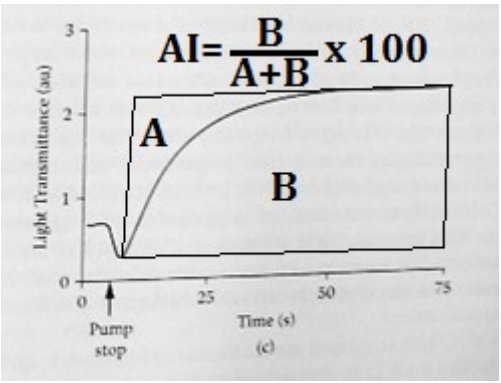

Figure 36 Aggregation index using Light Transmittance, modified from [28].

The main drawback with the light transmittance is that the technology has not left the research setting. These methods leave room for a clinical method which could be performed in less than 2 hours to provide rapid results.

4.1.3 Definition of a reactance aggregation index

The electrical impedance of blood relies upon the resistance of the plasma, and the number and orientation of the suspended RBCs. The RBCs have cell membranes, which act as capacitors, so that varying the input frequencies changes the impedance of the overall system. It is the capacitive effect of the RBCs, along with their orientation, that creates the changes in impedance used to detect blood aggregation.

For the purposes if these experiments, reactance was the measured value instead of capacitance. Reactance is related to capacitance by Equation 3, where A is any inductive effects:

$$Reactance\ (X) = A - \frac{1}{2\pi f C} \qquad \textit{Equation 3}$$

The aggregation of RBCs will change the overall impedance and reactance of the solution. For the impedance, the solution becomes mostly plasma as the blood cells aggregate, and therefore the overall impedance drops. The reactance should drop as well, and approach zero since all the capacitance of the RBC membranes is no longer in the current path. This approach towards zero makes it a preferable unit of measurement over total impedance since it will be more sensitive to any aggregation [11].

Recording the change of reactance and Impedance over 2 minutes after pump stop, during aggregation phase, will give information of the aggregability of the blood sample. The variation of impedance and capacitance can be plotted as a function of the time as presented Figure 37 , as was seen for light transmittance in section 4.1.2

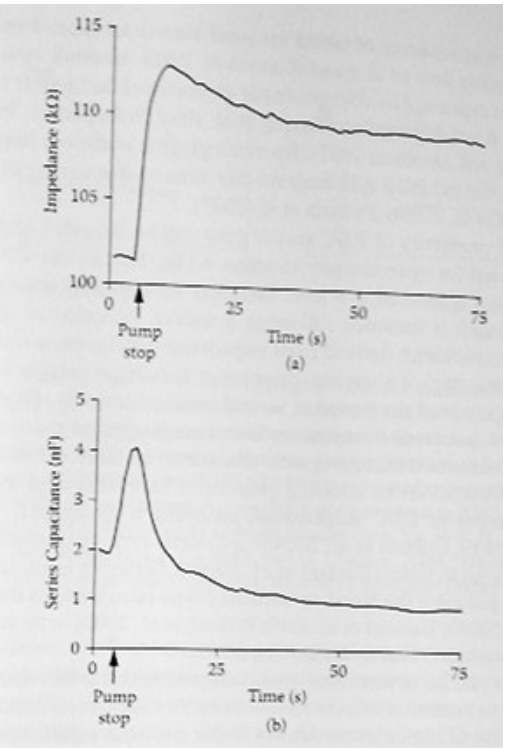

Figure 37 A comparison of impedance and capacitance values for measuring aggregation. Plots reproduced from [11].

In order to determine a capacitance aggregation index (AI_C), the reactance time course data will be used. The current standard, for light transmittance, is to use 2 minutes of data just after the blood has begun to settle, then calculate the area under the resulting curves. For reactance the aggregation index (AI_C) is calculated as,

$$AI_c = \frac{A}{A+B} \times 100 \text{ [11]} \qquad \textit{Equation 4}$$

where A and B are shown on Figure 38.

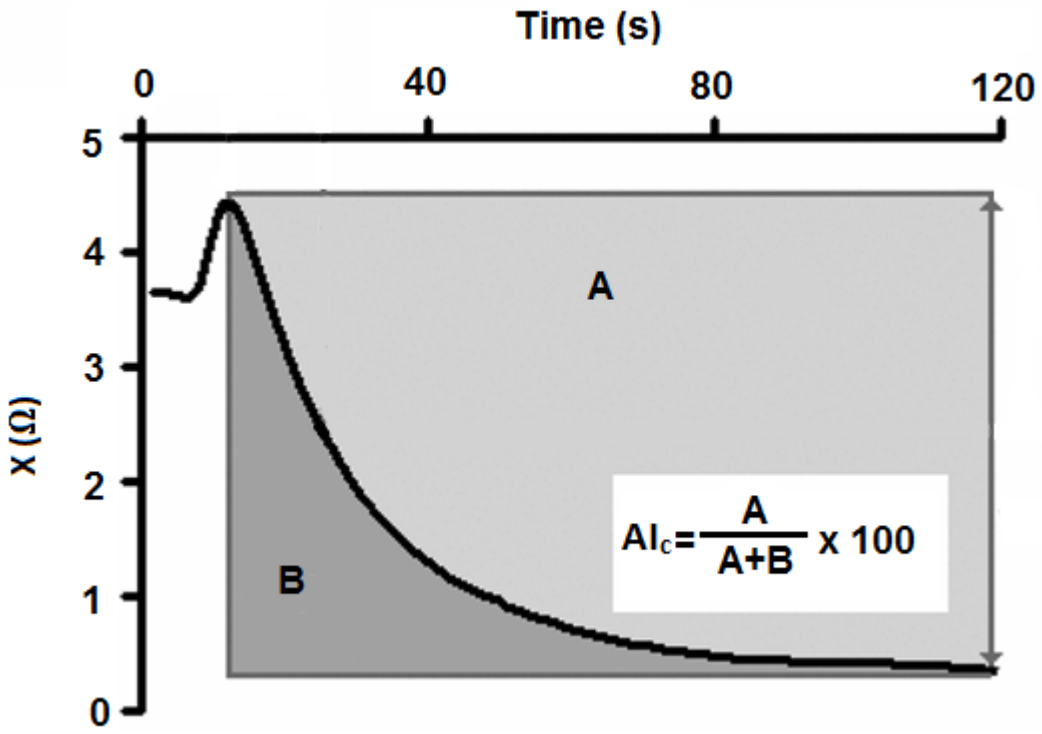

Figure 38 Aggregation index (AI_c) calculations using the areas bounded by the plot of capacitance change over time. Modified from [11].

The measured change in capacitance, along with the equation for AI_c give a quantitative method to calculate the aggregation index using electrical bioimpedance.

In order to measure the capacitance, a frequency is needed that will incorporate the membrane capacitance into the circuit model. If the frequency is too low, the current will not go through the cells, and therefore no capacitance will be measured. If the frequency is too high, the current will pass through the cells with no impedance from the membrane and will read a starting capacitance value near 0. Typically higher frequencies should be used, since they pass through the membrane and will still give a capacitance value.

4.1.4 Prior Research in RBC Aggregation

The electrical properties of blood are well known. Research dating back to the early 90's has been showing the effects of flow, hematocrit and other factors on the electrical impedance [28]. The variance between different samples of blood creates difficulty in isolating one important factor. This inability to isolate a single factor is the main hurdle for the use of electrical impedance for detecting aggregation.

Beving et al. in 1994 showed results for the settling of human red blood cells using electrical impedance that concluded that the measured transient in the cellular membrane capacitance suggests aggregation rather than a continuous settling process [31]. This was the first evidence that the aggregation of red blood cells exhibited a change in capacitance of the solution. With the correlation between capacitance and red blood cells established, researchers focused on isolating this relationship and comparing it to methods already in practice.

In 2004, *Pop et al.* [32] used electrical bioimpedance to measure blood aggregation *in vivo* using a catheter inserted into an anesthetized pig. Using 20 kHz frequency, they were able to measure the resistance and capacitance in pulsatile flow and found that blood aggregation was the main cause of the increase in blood viscosity under low shear conditions. As well, blood aggregation was also the main cause of electrical resistivity [32]. The measured viscosity change, correlating to the electrical resistance change,

was used to estimate the aggregation of red blood cells *in vivo* and during pulsatile flow. However, the values obtained were never converted into an AI or compared with any other form of aggregation measurement.

Antonova and Riha in 2006 [33] and *Baskurt et al.* in 2010 [11] demonstrated the relationship between frequency, hematocrit and aggregation readings. Frequencies ranging between 42 Hz and 2 MHz showed that the impedance varied greatly based on the solution and its state (flow or stasis).

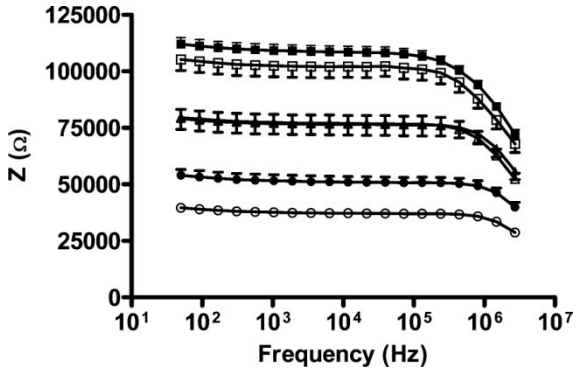

Figure 39 The effect of frequency on the impedance. Undiluted plasma during flow (□) and after 120 s after flow stoppage (■) as measured at frequencies between 42 Hz and 2.7 MHz. RBCs suspended in PBS was measured flow (Δ) and at stasis (◢). Lastly cell-free PBS (◦) and undiluted plasma (•) at stasis, reproduced from [11].

The data from Figure 39 shows large variability in the impedance as a function of state and suspending fluid. As a result, it was determined that the solutions must be controlled with respect to their hematocrit and their state [28] [11]. On top of that, a frequency must be picked to work across all the solutions. For this, *Baskurt et al.* used 100 kHz, since it maximized the changes in C and Z during the transition from flow to stasis [11].

Baskurt et al. in 2010 [11] published work comparing electrical impedance to light transmittance in terms of the AI. The set-up used a 75mm glass tube containing blood to measure the AI with light

transmittance and electrical impedance simultaneously. Using blood suspended in various substances, they compared the AI values for electrical impedance and light transmittance.

Using human blood, and a frequency of 100 kHz, *Baskurt et al.* was able to find similarities between electrical impedance and light transmittance. By comparing the light transmittance (LT), impedance (Z) and capacitance (C), they found that the C value remains similar to LT, especially for undiluted plasma.

Table 7 Aggregation parameters using LT, Z and C. Reproduced from [11].

LT	SA	AI	$T_{1/2}$ (s)
1/2 diluted plasma	12.8 ± 3.5	63.2 ± 3.3	21.5 ± 2.2
1/3 diluted plasma	31.5 ± 3.7	74.1 ± 2.8	16.5 ± 0.6
Plasma	100.6 ± 12.7	78.4 ± 1.5	11.7 ± 1.1
Plasma + 1% D500	153.0 ± 9.9	80.1 ± 1.5	10.8 ± 0.8
Z	SA	AI	$T_{1/2}$
1/2 diluted plasma	253.0 ± 23.3	59.6 ± 1.5	24.0 ± 1.8
1/3 diluted plasma	398.7 ± 18.1	68.7 ± 2.3	16.0 ± 1.9
Plasma	204.3 ± 28.6	73.8 ± 2.5	10.1 ± 0.8
Plasma + 1% D500	207.6 ± 34.2	69.8 ± 5.3	12.2 ± 1.7
C	SA	AI	$T_{1/2}$
1/2 diluted plasma	27.1 ± 1.5	60.6 ± 5.1	21.5 ± 1.0
1/3 diluted plasma	41.2 ± 16.6	67.3 ± 2.8	12.7 ± 2.2
Plasma	81.1 ± 10.6	79.0 ± 1.7	8.8 ± 1.3
Plasma + 1% D500	131.0 ± 17.6	84.4 ± 1.8	10.9 ± 1.2

Z and *C* were monitored at 100 kHz frequency. Data are mean ± SE.

From Table 7, for the accuracy of C with respect to LT, the error ranges from 0.7 to 9.2%, with the most accurate AI being the undiluted plasma at 0.7%.

The choice of the electrical frequency is important. The electrical frequency would change the aggregation index measured, based on its sensitivity to aggregates forming. Its sensitivity will change the slope of the curve shown in Figure 38, and give a new areas under the curve. These areas create an AI which is not the accepted value for the blood using current detection methods. Despite this, we

hypothesize that a more sensitive frequency is ideal since it will detect minor differences in AIs. The best scenario would be to use a highly sensitive frequency and convert its AI to the more standard value.

Current experiments by *Baskurt* [11] use 100 kHz as it conforms to the medical fields' value for aggregation [11] [28]. These measurements with 100 kHz using the change in capacitance over the 120 second time were able to get accuracy to within 9.5% or better with the standard AI measurements [11]. An additional justification was given for 100 kHz as the amplitude of Z and C were at a maximum at 100 kHz. This emphasizes the effect of Z and C and makes a compromise between the two, however it was shown that Z does not follow the AI well [11]. As a result, maximizing the sensitivity of capacitance to blood aggregation is a necessary step in these experiments.

4.1.5 Conclusion of Literature Review

The prior work done with electrical bioimpedance and blood aggregation show a link between the capacitance and the AI. This link will be exploited to create a set-up capable of rapidly detecting the AI at a sensitive frequency. The goal of the experiment is to perform experiments using a clinical device at a frequency which maximizes the sensitivity of capacitance to blood aggregation. We hypothesize that at a sensitive frequency, the Z-Metrix will be able to detect the aggregation of blood and using the method similar to the light transmittance model, will be able to rapidly produce an AI for the measured blood.

To maximize the sensitivity, electrical impedance spectroscopy will be performed for a range of frequencies (2 to 304 kHz) during the aggregation process. The frequency that shows the highest sensitivity for the capacitance to blood aggregation will be chosen as the ideal frequency. Experiments will be performed using the Z-Metrix and this new frequency to measure the capacitance change and calculate an aggregation index.

4.2 Materials and Methods

4.2.1 Materials

All experiments are being performed using a function generator and receiver from BioParHom (*Z-Matrix*). The function generator has 2 output cables (R and R') to close the circuit and 2 leads (C and C') to measure the signals. These 4 cables are connected to a custom 4 electrode probe. The electrodes are made of stainless steel and are spaced 10 mm apart (for a total of 30 mm in length), shown in Figure 41. All functions are run through a computer connected by USB to the function generator. Using *ZFlow* by Bioparhom, the function generator is controlled to run at set signal frequencies and durations.

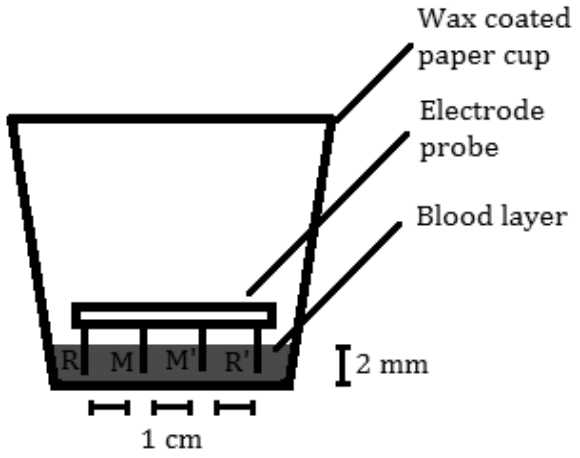

Figure 40 Schematic showing the blood, blood container and electrode probe..

The blood is from American Yorkshire pigs, anticoagulated with 2 mg/ml Ethylenediaminetetraacetic acid (EDTA) in 8 ml/l of diluted water. The blood is contained in a wax sealed paper cup (*Dixie* cup), shown in Figure 41.

Figure 41 Diagram showing the cup dimensions with blood.

4.2.2 Methods

Initially, blood is brought to room temperature (20^0C). The function generator is attached to the computer and the custom probe. The *ZFlow* is run and in the software, the test frequency is specified (100 kHz, 304 kHz or spectroscopy depending on the experiment being run), and the duration is set at 120 seconds.

The blood is agitated gently for 10 seconds to suspend the RBCs. 2 ml of blood is isolated and placed within the wax sealed cup. Immediately after the blood is placed in the cup, the probe is placed inside the blood and the software is run.

These tests are repeated 3 times for blood taken from each pig to test the precision of the results.

4.2.2.1 Hematocrit Methods

To calculate the hematocrit of the blood the following procedure was followed. A small sample of blood (approximately 1-2 ml) was placed within a capillary micro-hematocrit tube. This sample was centrifuged in a *CritSpin Hematocrit Centrifuge* (*StatSpin*) for 120 seconds at 16,000 rpm.

After spinning, the blood separates and the percentage of red blood cells can be seen visibly. This visible percentage is the hematocrit, shown in Figure 42.

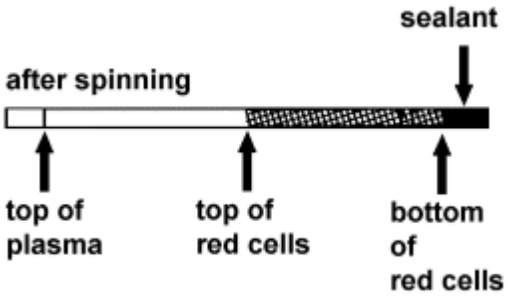

Figure 42 Representation of the hematocrit in a micro-hematocrit tube [34].

Viscosity measurements were performed using the different blood samples and running them through a viscometer *(uVISC™ Portable Viscometer)*. Samples were tested at shear rates of 50, 200, 500 and 1000 s^{-1}. The viscosity curves were created from the results.

4.2.3 Statistical and Analytical Methods

To calculate an AI value using reactance of blood, a curve is plotted over 2 minutes. Afterwards, the area under and over the plot are calculated and compared. This comparison gives the AI similar to the method used by light transmittance.

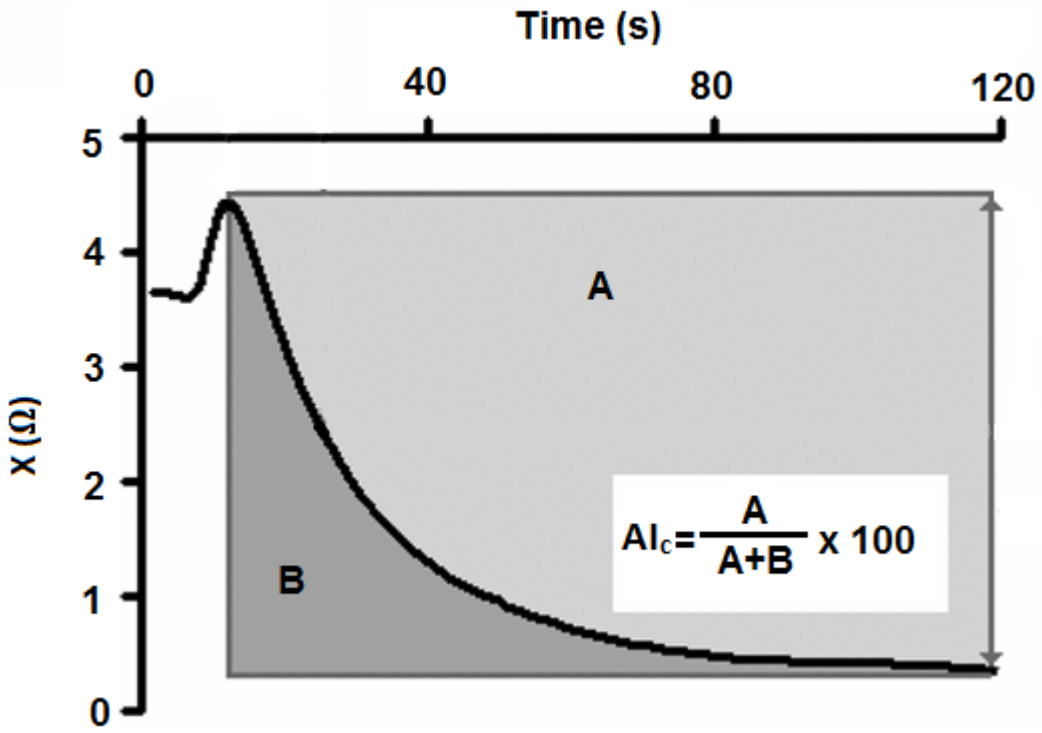

Figure 43 The reactance method to calculate the AI. The shaded areas represent the measured areas above and below the curve, modified from [11].

This method is then compared to the physiological values for porcine blood (3-30%).

Multiple trials are run on blood from the same pig. These AIs are evaluated using the standard deviations to measure the precision of the frequency used for the AIs. The lower the standard deviation, the closer the measured AIs are to one another for a given pig sample. This is a method to compare the validity of different frequencies. Minimizing the standard deviation for a given pig blood is desired.

The Power Law, also known as the Ostwald Model follows Equation 5.

$$\mu = \mathrm{K}(\dot{\gamma})^{n-1} \qquad \textit{Equation 5}$$

The power law model fits the viscosity (μ) to the shear rate ($\dot{\gamma}$). This creates a model that closely follows the viscosity plots for blood. A non-linear model is used because blood is a non-Newtonian fluid and does not respond linearly to shear. Utilizing the constants from the power law, a correlation can be drawn to

the aggregation index of the pig blood. This is a secondary test to strengthen the relationship between the reactance AI and the physiological AI.

Equation 5 is derived from the more common form of:

$$\tau = K(\dot{\gamma})^n \qquad \textit{Equation 6}$$

where τ is the shear stress. Since the shear stress is related to viscosity by $\tau = \dot{\gamma}\mu$, we can substitute viscosity into Equation 6 to get Equation 5.

The results gives two coefficients, the Power Law Index (n) and the Consistency (K). The Power Law Index is a measure of how non-Newtonian a fluid is. For blood, a shear thinning fluid, a value between 0 and 1 is expected. The Consistency is the starting value of the curve, found at a shear rate of 1 s^{-1} [35].

4.3 Results and Discussion

4.3.1 Impedance Spectroscopy

A sample of the impedance spectroscopy results can be seen in Figure 44. This sample shows the difference in reactance and resistance as a function of frequency between time intervals 0 and 1 minute.

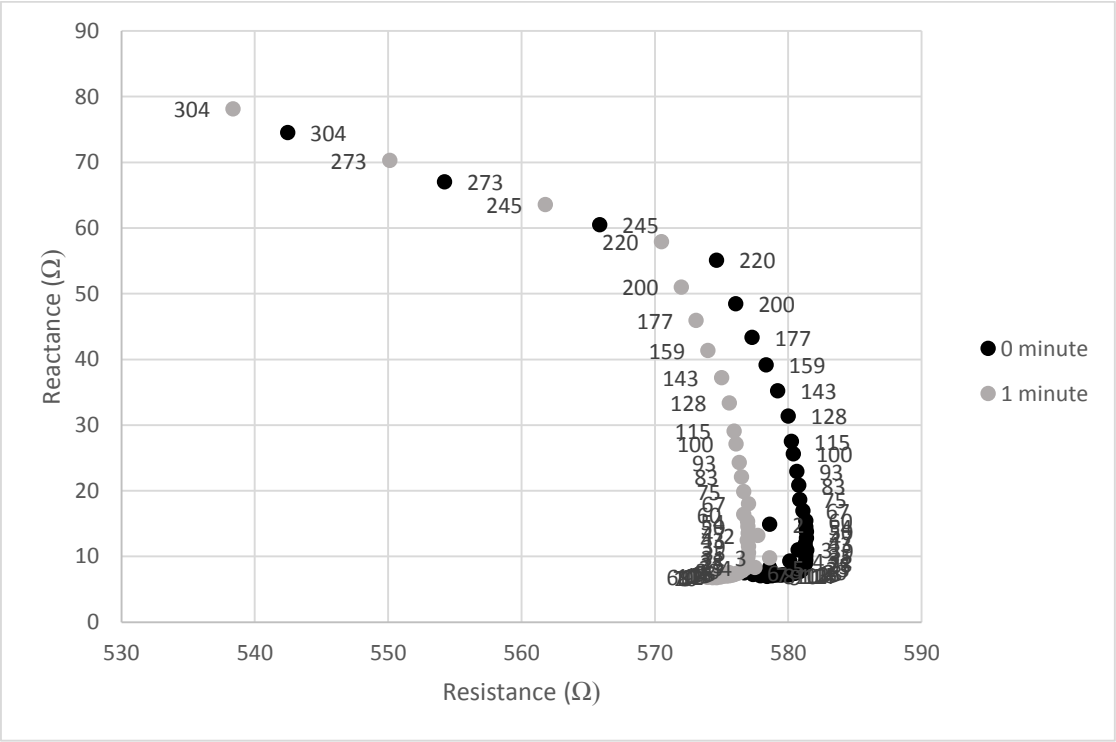

Figure 44 Impedance Spectrum for Pig blood sample VII. The values represent frequencies in kHz.

Showing a close up of the lower frequency values (6-75 kHz) for clarity creates Figure 45.

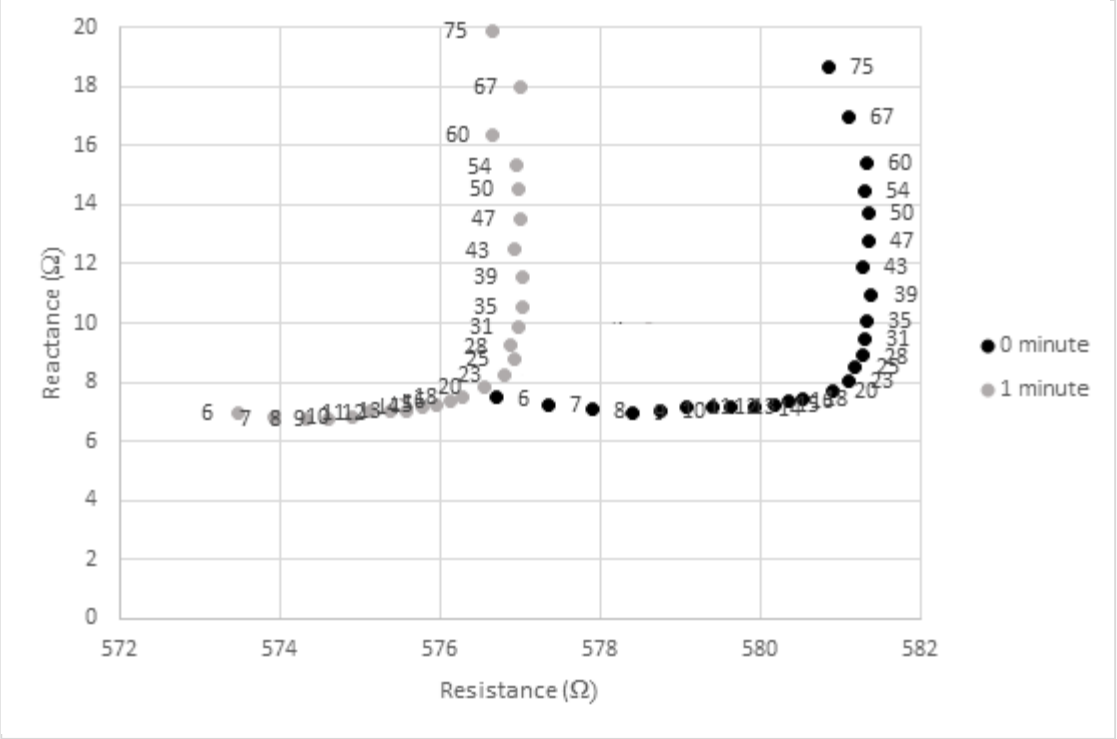

Figure 45 Impedance spectrum for pig blood sample VII enlarged to show frequencies between 6 to 75 kHz. The numbers represent frequencies in kHz.

The difference between the reactance values for each timestamp (0 or 1 minute) and the difference in resistance values at each frequency were then plotted to show the frequency with the highest sensitivity. The sensitivity, shown in Equation 7, which is the scalar difference in reactance or resistance between time 0 and 1 minute, with the frequency, is presented in Figure 46.

$$sensitivty = |reactance(0) - reactance(1)| \quad \textit{Equation 7}$$

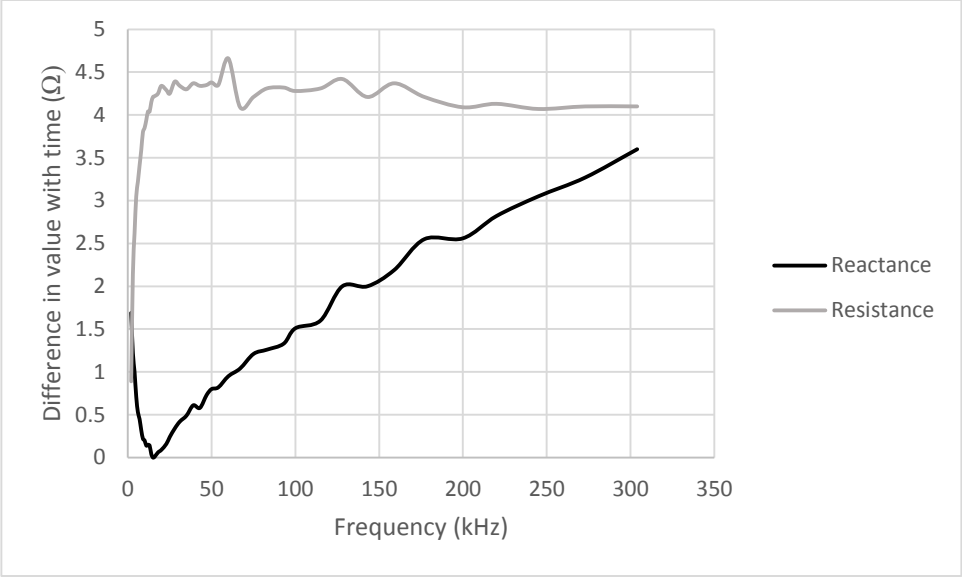

Figure 46 The sensitivity for reactance and resistance plotted against frequency for pig VII.

Since we are trying to maximize the sensitivity of the reactance change to blood aggregation, the higher frequencies are better suited to measure the aggregation index. As seen in Figure 46, a frequency of 304 kHz has the highest difference in reactance, and is therefore the most sensitive frequency tested.

Averaging all of the 11 data sets from 5 different pigs, and representing the sensitivity of the reactance function of the frequency, we get the following plot, Figure 47.

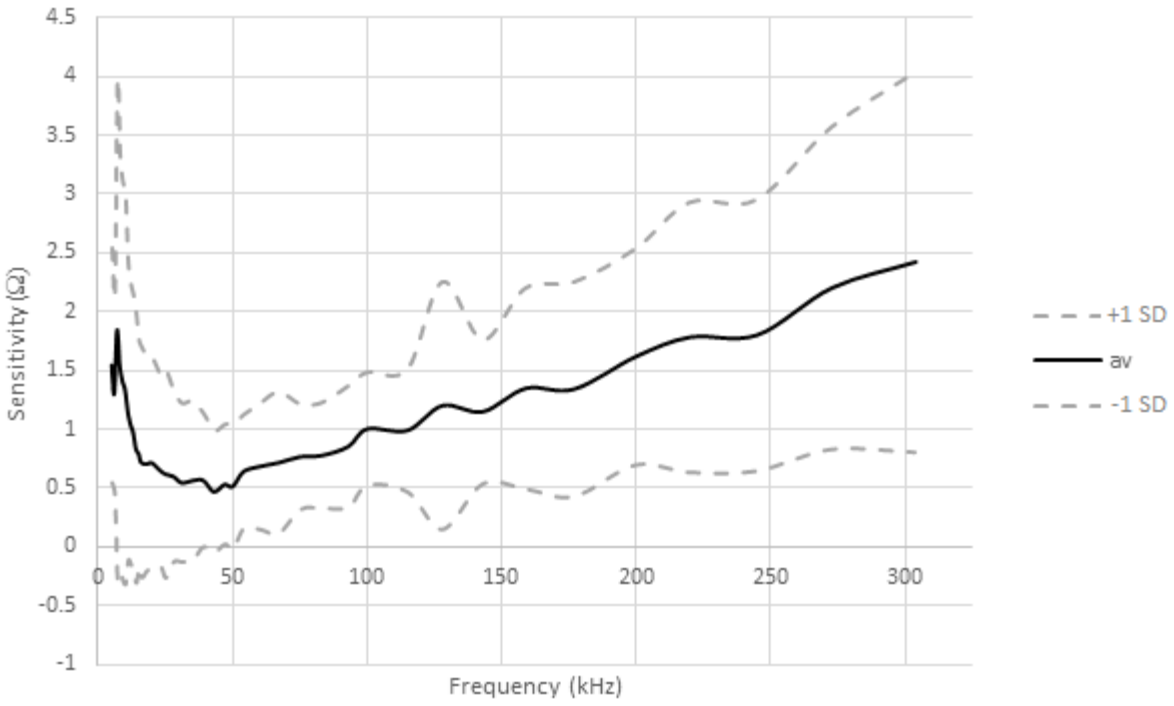

Figure 47 Spectrum of the Sensitivity of the Reactance to blood aggregation (5-304 kHz). ± 1 SD values are 1 Standard Deviation from the average.

What was seen with Figure 47 is that at frequency of 304 kHz, the difference in reactance is at a maximum. Therefore, for the following experiments calculating the aggregation index, a frequency of 304 kHz will be used.

4.3.2 Aggregation Index Results and Discussion

For the measured AI_c, results were taken at a frequency of 304 kHz for 3 different pigs. The curves followed a general shape shown in Figure 48.

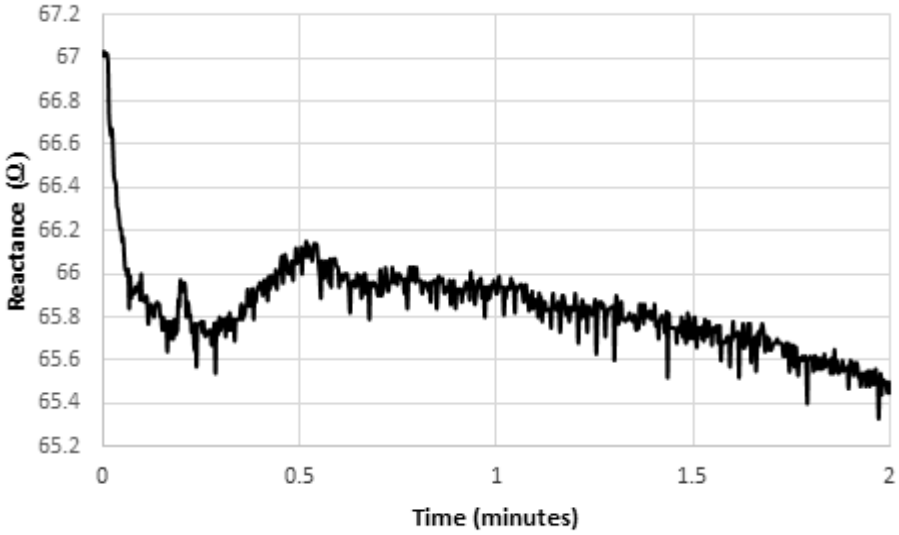

Figure 48 General shape of the reactance change with aggregation, taken from pig X (304 kHz).

Highlighting the areas of the graph shown in Figure 48, we get Figure 49.

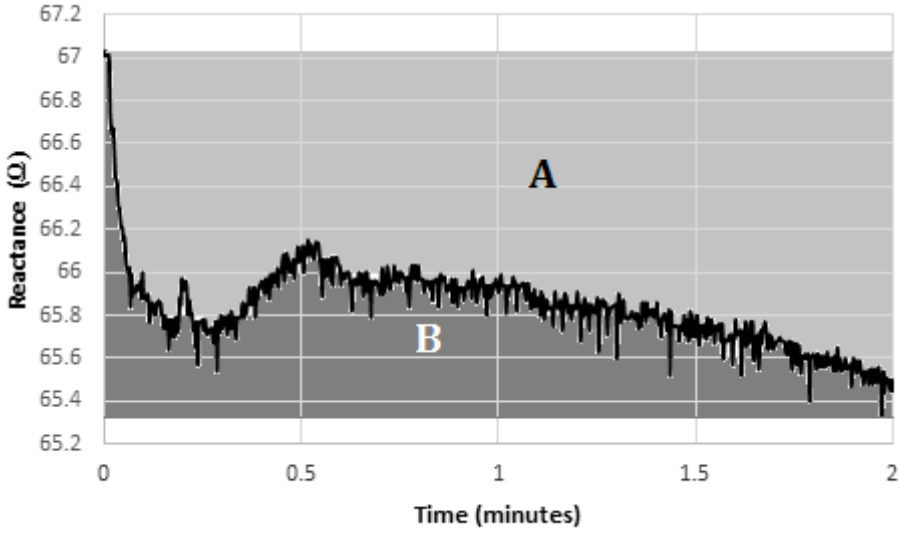

Figure 49 Plot showing the shaded areas used to calculate the AI_c.

To calculate the AI, we use Equation 4 from section 4.1.3:

$$AI_c = \frac{A}{A+B} \times 100\%$$

As an example, with the areas in Figure 49, of $A = 932.86$ and $B = 399.94$, we get an AI_c of 70.

The AI_cs for all the experiments at 304 kHz are shown in Table 8. The sample column represents different samples of blood taken from the same pig, to test precision. The AI_C value is the calculate aggregation index described earlier. The average values also shows a ± standard deviation. The H value is the hematocrit of the pigs' blood, which is the percentage of red blood cells in a sample of blood by volume (expected to be around 40% from physiology).

Table 8 The results of the AI_c from three pigs at 304 kHz.

Pig	Sample	AI_c	Average AI_c	H
Pig X	1	36.26	43±20	39
	2	70		
	3	22.79		
Pig XI	1	28.76	37±8	41
	2	35.75		
	3	47.52		
Pig XII	1	14.31	16±5	41
	2	10.84		
	3	22.33		

Aside from pig X, the other blood samples shows little variability. Porcine blood has lower AI_c values than human blood, ranging from 3-30 [36]. The 304 kHz frequency was able to extract physiological values.

The largest aggregation growth was seen in pig X, and is correlated with the largest average AI_c shown in Table 8. What is also seen in Table 8 is that the standard deviation for pig XI and XII stays relatively small, meaning there is good precision in the 304 kHz frequency.

All of the aggregation comparisons are shown in a high contrast image set found in Table 9. The white is any gaps between the red blood cells, and an increase in white shows an increase in aggregation. This helps visually represent the AI_c in pig XI, which experiences aggregation in a large number of smaller aggregates. An increase in white from the first to second image represents more aggregation for a given pigs blood.

Table 9 High contrast diagram highlighting the aggregation found in each pig blood sample at 304 kHz. The images were taken at 0 minutes and 2 minutes following agitation to show aggregation.

Pig	T = 0 minutes	T = 2 minutes
Pig X	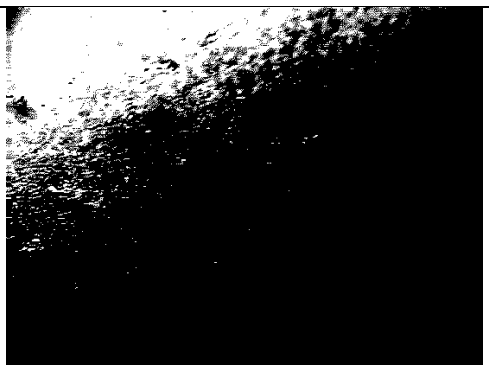	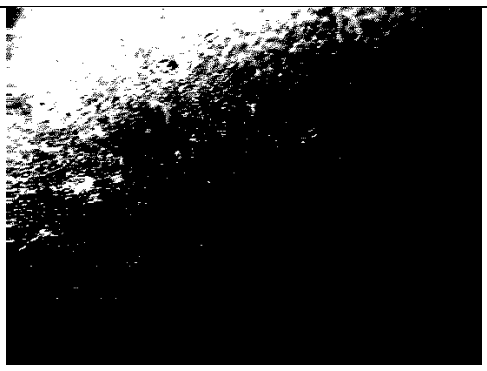
Pig XI		

Pig XII

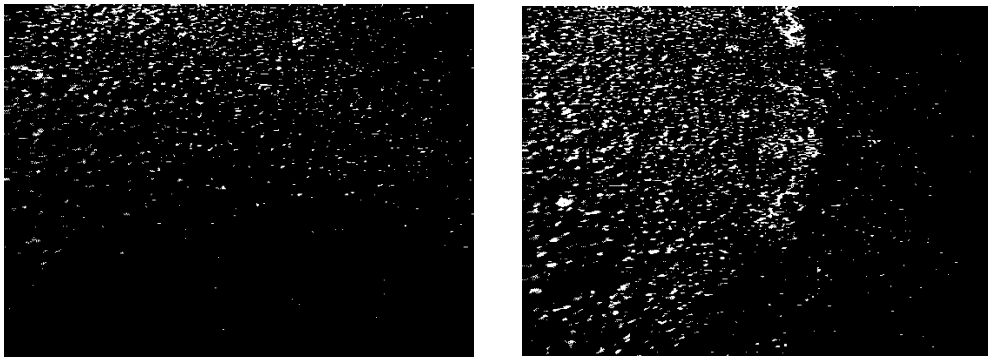

The viscosities plotted in Figure 50 show two distinct regions in each curve. The first region is the more vertical region, which is explained by the separation of blood aggregates. The second part of the curve, the linear region, is due to the blood cells deforming.

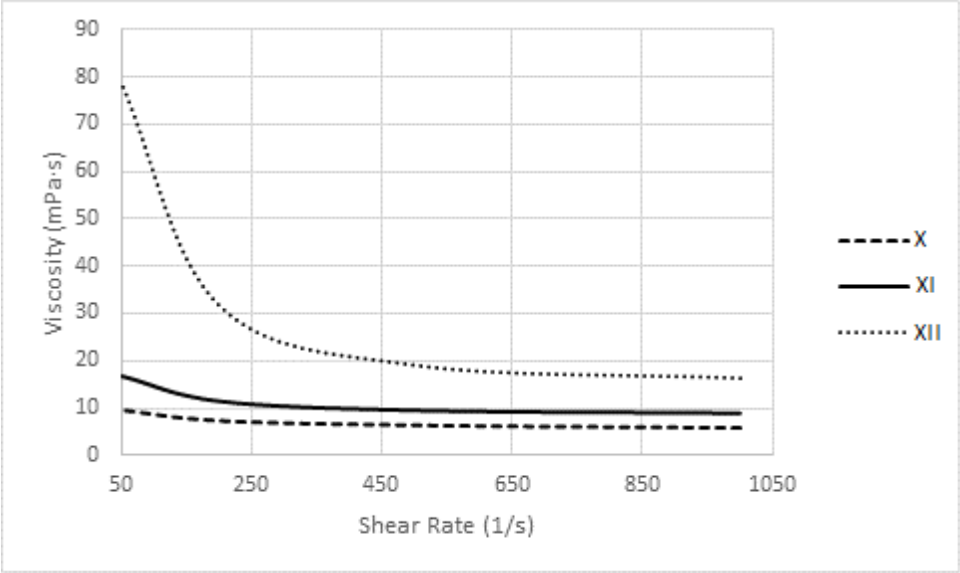

Figure 50 Measured viscosities of the blood samples for pigs X, XI, XII.

From the viscosities plotted above, using the power law described in section 4.2.3 ($viscosity = K(shear\ rate)^{n-1}$), we get the coefficients for blood I-III as the following:

Table 10 Power law coefficients and correlation to viscosity curves in Figure 50.

Pig	Coefficient (K)	Power Law Index (n)	Correlation (R)
Pig X	17.1	0.844	0.997
Pig XI	37.8	0.784	0.985
Pig XII	712.7	0.459	0.988

Table 10 shows good correlation of the power law to the measured viscosity curves. n shows correlation to the measured average AI_c for pigs X, XI and XII, presented in Table 8. All the power law index values (n) were between 0 and 1, which was expected for blood. What is shown is that based on the viscosities we expect pig X to have the highest aggregation index since its n value is the highest, and pig XII to have the lowest AI since its n value is the lowest. This relationship shows that the experiments run are self-consistent, in that the measured AI corresponds to the expected AI. This does not describe the validity of the measured value, just that high AIs are properly measured to be higher than low AIs.

At 100 kHz, the calculated values for AI_c have a higher variability than presented in the 304 kHz data.

Table 11 The results of the AI_c from 3 pigs at 100 kHz.

Pig	Sample	AI_c	Average AI_c
Pig VII	1	54.92	38±18
	2	12.77	
	3	47.7	
	1	32.7	

Pig VIII	2	69.11	49±15
	3	45.1	
	1	59.8	
Pig IX	2	32.1	36±18
	3	17.4	

Table 11 shows the variability and the values presented using 100 kHz to measure the reactance. The standard deviations for 100 kHz are higher than those for 304 kHz shown in Table 8.

The values for 100 kHz AI's were of the same magnitude as those measured at 304 kHz. This means that there can be correlation of the 304 kHz values to the light transmittance method as was described by *Baskurt et al* [11]. The difference in the data sets come mostly from the reproducibility of the data. All of the standard deviations for the 100 kHz data were above 14, while at 304 kHz only 1 data set was above 8. This lower standard variation at 304 kHz is an advantage of the higher frequency.

Due to the smaller standard deviations and the correlation to the visual data, the use of 304 kHz provided a better precision and accuracy for measuring the aggregation index of porcine blood than 100 kHz. As well, the method and technology were able to measure an aggregation index within physiological bounds, making this an early justification for the use of electrical bioimpedance as a measurement tool for AI.

4.3.3 Discussion of Experimental Setup

4.3.3.1 Blood Characteristics

For aggregation, porcine blood was used. Porcine and human blood have similar characteristics. This similarity gives results, consistent with human blood results, when performing the experiments on porcine blood [14]. At constant hematocrits and temperature, the binding forces and structure of human

and pig RBCs are similar, and the aggregation levels change for both when the blood is diluted. It was therefore concluded that porcine blood was an appropriate replacement for human blood for aggregation experiments.

The volume of blood used in the experiment was a balance of two characteristics: minimizing the necessary amount and making the tests simple and repeatable. The use of the smallest quantity of blood is to require the smallest amount from any potential patient. If a drop or less is needed, it is more favorable than a large volume since only a pin-prick would be required from the patient.

4.4 Conclusion and Future Work

It was found that the reactance changes, measured with the Z-Metrix, were capable of calculating an aggregation index within physiological limits. This early work showed the potential of the used of electrical bioimpedance to measure the aggregation index in a fraction of the time of the current sedimentation method.

Following a method used in light transmittance, and the principles outlined *Baskurt et al.* [11], the area subtended from the capacitance drop due to blood aggregation was used to calculate an aggregation index. The index found for porcine blood, as hypothesized was within the physiological ranges expected.

Future work to minimize the set up and amount of blood needed would allow for a point-of-care device. Using a more specialized blood container and electrodes with smaller distances would reduce the 2 ml of blood used in the experiments. This would improve comfort for a patient.

A well, future work would include using an aggregometer and the light transmittance to validate the results. This would show a correlation to the previous work of *Baskurt et al.* and also justify the research for finding a physiological AI.

The potential for *in vivo* experiments would allow for bed side results. Utilizing the ability of electrical signals to penetrate the skin, experiments could be run on blood vessel with aggregation forming when the vessel is pinched to stop flow for 2 minutes. This would reduce any need to extract blood, and give the care provider rapid results.

It was shown that the Z-Metrix was capable of detecting the reactance changes in aggregating blood, and a physiological aggregation index was found for small quantities of blood within 2 minutes using electrical bioimpedance at 304 kHz.

5 Conclusion

The main objective of this research is to improve upon and develop new applications, using bioimpedance. The use of electrical bioimpedance as a measurement tool was shown to be capable of detecting fluid indicators. The early stage proof of concept experiments to validate the use of the Bioparhom Z-Metrix for clinical applications were performed. The macro-scale pooling of blood within a deceased rat abdomen was detected and located, while the micro-scale aggregation of red blood cells was quantified. For both experiments, the unique application of the device was tested, as well as the evaluation of the frequencies used by previous researchers for optimized results.

The detection of blood pooling within a rat abdomen, mimicking internal bleeding, was detected using a 4 electrode set-up at a low frequency of 5 kHz. 5 and 95 kHz were chosen due to the prevalence of those frequencies in literature. 5 kHz was found to be more sensitive to blood pooling since it accentuated the effect of the blood plasma since the current was unable to penetrate the cell membranes of the tissue. Blood plasma has a low resistance, so the presence of blood pooling was found to decrease the paths resistance over time. A low correlation of determination was found. This was due to the horizontal nature of the regression line, along with a high number of data points. Physiological flow rates and volumes were used and, despite the low correlation, blood pooling was detected using this method.

The localization of blood pooling was achieved using an electrode grid and cycling through a series of current paths. Paths experiencing a decrease in resistance contain some of the pooled blood. From this, a graphical display was created which matched with the bruising seen in several of the rats. This provided a general region where the blood pooling was occurring with the greatest rate.

Blood aggregation was quantified using an aggregation index at a high frequency. Despite the more commonly used frequency of 100 kHz, it was found that a higher frequency of 304 kHz was more sensitive to aggregation. Due to this heightened sensitivity, experiments were run at 100 and 304 kHz,

measuring the reactance change of blood over 2 minutes. Based on the relative areas above and below the curve, an aggregation index was found and compared to normal physiological values for pigs, as well as with graphic representation of the blood aggregating. The measured aggregation index matched with the graphic representation, and was found to be within expected physiological ranges for 304 kHz, and outside of the range for the 100 kHz experiments.

The ability to measure macro and micro-scale blood indicators with electrical bioimpedance is important since electrical bioimpedance can provide rapid, real-time *in vivo* results. This can provide physicians with readily available data which could help the earlier diagnosis of potentially fatal conditions. The evaluation of the frequencies, the use of a novel device along with the multipurpose nature of the device provide a unique insight into the clinical applications of electrical bioimpedance.

Future work for the blood pooling detection will look at improving and automating the visual localization plot by refining the algorithm used. Developing a calibration factor to relate the resistance drop to the blood pooling rate will also be created with the goal of determining the severity of the bleeding. Lastly, scaling the system for human use will be done.

For the blood aggregation, minimizing the set up and amount of blood needed through specialized containers and redesigned electrodes will allow for a point-of-care device. Lastly, using an aggregometer and the light transmittance will help to validate the results.

It was found that electrical bioimpedance was capable of detecting and locating blood pooling within a rats abdomen with a higher sensitivity at 5 kHz, and was also capable of quantifying the aggregation of red blood cells at a higher frequency than previously used of 304 kHz.

References

[1] S. Grimnes and O. Martinsen, Bioimpedance and Bioelectricity Basics, Academic Press, 2000.

[2] H. Fricke and S. Morse, "The electric resistance and capacity of blood for frequencies between 800 and 4 1/2 million cycles," *The Journal of General Physiology,* pp. 153-67, 1925.

[3] E. McAdams and J. Jossinet, "Tissue impedance: a historical overview," *Physiological Measurements,* vol. 16, pp. A1-13, 1995.

[4] K. S. Cole, "Electrical impedance of suspensions of spheres," *Journal of General Physiology,* vol. 12, no. 1, pp. 29-36, 1928.

[5] R. Hober, "Eine method, die elektrische Leitfahigkeit im Innern von Zellen zu messen," *Pflüger's Archiv für die gesamte Physiologie des Menschen und der Tiere,* vol. 133, no. 4-6, pp. 237-53, 1910.

[6] J. G. Webster, Medical Instrumentation: Application and Design, 4th ed., John Wiley & Sons Inc., 2010.

[7] R. Sadleir, R. Fox, F. van Kann and Y. Attikiouzel, "Estimating volumes of intra-abdominal blood using electrical impedance imaging," in *Engineering in Medecine and Biology Society*, 1992.

[8] T. Krantz, Y. Cai, T. Lauritsen, J. Warberg and N. Secher, "Accurate monitoring of blood loss: thoracic electrical during hemorrhage in the pig," *Acta Anaesthesiologica Scandinavica,* vol. 44, 2000.

[9] S. Wanjun, Y. Fusheng, Z. Wei, Z. Hongyi, F. Feng, S. Xuetao, L. Ruigang, X. Canhua, D. Xiuzhen and B. Tingyi, "Image monitoring for an intraperitoneal bleeding model of pigs using electrial impedance tomography," *Phyisiological Measurement,* vol. 29, pp. 217-25, 2008.

[10] G. Blumrosen, C. A. Gonzalez and B. Rubinsky, "New wearable body sensor for continuous diagnosis of internal tissue bleeding," in *Wearable and Implantable Body Sensor Networks, 2009*, Berkley, CA, 2009.

[11] O. Baskurt, H. J. Meiselman and M. Uyuklu, "Time Course of Electrical Impedance During Red Blood Cell Aggregation in a Glass Tube: Comparison with Light Transmittance," *IEEE Transactions on Biomedical Engineering,* vol. 57, no. 4, pp. 969-978, 2010.

[12] S. S. Nathan, S. R. Sinha, B. Gordon, R. P. Lesser and N. V. Thakor, "Determination of current density distributions generated by electrical stimulation of the human cerebral cortex," *Electroencephalography and clinical Neurophysiology,* vol. 83, pp. 183-92, 1993.

[13] S. L. Goodman, "Sheep, pig, and human platelet–material interactions with model cardiovascular biomaterials," *Journal of Biomedical Materials Research,* vol. 45, no. 3, pp. 240-250, June 1999.

[14] X. Wang, G. Cloutier, P. Pibarot and L. G. Durand, "Comparison and simulation of different levels of erythrocyte aggregation with pig, horse, sheep, calf, and normal human blood," *Biorheology,* vol. 33, no. 4-5, pp. 365-77, Jul-Oct 1996.

[15] D. A. Heltrick and T. M. Zielinski, "Bioimpedance in Cardiovascular Medicine," in *Encyclopedia of Medical Devices and Instrumentation*, 2006.

[16] L. A. Geddes and H. Kidder, "Specific resistance of blood at body temperature II," *Medical and Biological Engineering,* pp. 180-5, 1976.

[17] B. Wedro, "Medicine Net," [Online]. Available: http://www.medicinenet.com/internal_bleeding/. [Accessed 03 2012].

[18] John Hopkins Medicine, "John Hopkins University," [Online]. Available: http://www.hopkinsmedicine.org/healthlibrary/test_procedures/pulmonary/chest_ultrasound_92,P07748/. [Accessed 25 03 2013].

[19] W. A. Knaus, S. A. Schroeder and D. O. Davis, "Impact of New Technology: the CT Scanner," *Medical Care,* vol. XV, no. 7, pp. 533-42, 1977.

[20] R. Sadlier and R. Fox, "Quantification of blood volume by electrical impedance tomography using a tissue-equivalent phantom," *Physiological Measurement,* vol. 19, no. 4, pp. 501-16, 1998.

[21] R. J. Rummel, "Hawaii University," 1976. [Online]. Available: http://hawaii.edu/powerkills/UC.HTM. [Accessed 2013].

[22] Flowing Data, "Flowing Data," 15 February 2008. [Online]. Available: http://flowingdata.com/2008/02/15/how-to-read-and-use-a-box-and-whisker-plot/. [Accessed 2013].

[23] H. Lee and M. Blaufox, "Blood Volume in the Rat," *Journal of Nuclear Medecine,* 1995.

[24] J. Cameron, J. Skofronick and R. Grant, Physics of the Body, Medical Physics Publishing, 1999.

[25] S. Mao, F. Fu, X. Dong and Z. Wang, "Supplementary Pathway for Vitality of Wounds and Wound Age Estimation in Bruises Using the Electric Impedance Spectroscopy Technique," *Journal of Forensic Sciences,* vol. 56, no. 4, pp. 925-9, July 2011.

[26] A. V. Cardoso, M. H. Pereira, G. A. Marcondes, A. R. Ferreira and P. R. de Araujo, "Microplate reader analysis of triatomine saliva effect on erythrocyte aggregation," *Materials Research,* vol. 10, no. 1, pp. 31-6, 2007.

[27] C. P. Davis and M. C. Stoppler, "Medecine Net," [Online]. Available: http://www.medicinenet.com/sepsis/page6.htm. [Accessed 29 11 2012].

[28] O. Baskurt, B. Neu and H. J. Meiselman, Red Blood Cell Aggregation, CRC Press, 2012.

[29] R. R. Azar, "Should we Monitor Anti-Platelet Treatment?," 2011.

[30] T. Tabuchi, H. Tominaga and N. Tatsumi, "Problems related to rapid methods for erythrocyte sedimentation rate test and their solution," *Southeast Asian Journal Tropical Medicine Public Health,* vol. 33, no. 2, pp. 151-4, 2002.

[31] H. Beving, L. E. G. Eriksson, C. L. Davey and D. B. Kell, "Dielectric Properties of Human Blood and Erythrocytes at Radio Frequencies (0.2-10 MHz): Dependence on Cell Volume Fraction and Medium Composition," *European Biophysics Journal,* vol. 23, pp. 207-15, 1994.

[32] G. A. M. Pop, Z. Y. Chang, C. J. Slager, B. J. Kooij, E. D. van Deel, L. Moraru, J. Quak, G. C. M. Meijer and D. J. Duncker, "Catheter-Based Impedance Measurements in the Right Atrium for Continuously Monitoring Hematocrit and Estimating Blood Viscosity Changes: An In Vivo Feasbility Study in Swine," *Biosensors & Bioeletronics,* vol. 15, pp. 1685-93, 2004.

[33] N. Antonova and P. Riha, "Studies of Electrorheological Properties of Blood," *Clinical Hemorheology Microcirculation,* vol. 35, pp. 19-29, 2006.

[34] StatSpin Inc., *CritSpin Hematocrit Centrifuge: Operator's Manual,* 2004.

[35] N. Cunningham, "Rheology School," Brookfield Engineering Laboratories, 2013. [Online]. Available: http://www.brookfieldengineering.com/education/rheology_papers_benchmark_products.asp. [Accessed 2013].

[36] U. Windberger, A. Bartholovitsch, R. Plasenzotti, K. J. Korak and G. Heinze, "Whole blood viscosity, plasma viscosity and erythrocyte aggregation in nine mammalian species: reference values and comparison of data," *Experimental Physiology,* vol. 88, no. 3, pp. 431-40, 2003.